Regd. No. C-3911

VOL. 35 **INDIAN JOURNAL OF PHYSICS** No. 5

(Published in collaboration with the Indian Physical Society)

AND

VOL. 44 **PROCEEDINGS** No. 5

OF THE

INDIAN ASSOCIATION FOR THE CULTIVATION OF SCIENCE

MAY 1961

PUBLISHED BY THE
INDIAN ASSOCIATION FOR THE CULTIVATION OF SCIENCE
JADAVPUR, CALCUTTA 32

Annual Subscription—
Inland Rs. 25.00
Foreign £ 2-10-0 or $ 7.00

NOTICE
TO INTENDING AUTHORS

1. Manuscripts for publication should be sent to the Assistant Editor, Indian Journal of Physics, Jadavpur, Calcutta-32.

2. The manuscripts submitted must be type-written with double space on thick foolscap paper with sufficient margin on the left and at the top. The original copy, and not the carbon copy, should be submitted. Each paper must contain an Abstract at the beginning.

3. All References should be given in the text by quoting the surname of the author, followed by year of publication, *e.g.*, (Roy, 1958). The full Reference should be given in a list at the end, arranged alphabatically, as follows; Mazumder, M. 1959, *Ind. J. Phys.*, **33**, 346.

4. Line diagrams should be drawn on white Bristol board or tracing paper with black Indian ink, and letters and numbers inside the diagrams should be written neatly in capital type with Indian ink. The size of the diagrams submitted and the lettering inside should be large enough so that it is legible after reduction to one-third the original size. A simple style of lettering such as gothic, with its uniform line width and no serifs should be used, *e.g.*,

A·B·E·F·G·M·P·T·W·

5. Photographs submitted for publication should be printed on glossy paper with somewhat more contrast than that desired in the reproduction.

6. Captions to all figures should be typed in a separate sheet and attached at the end of the paper.

7. The mathematical expressions should be written carefully by hand. Care should be taken to distinguish between capital and small letters and superscripts and subscripts. Repetition of a complex expression should be avoided by representing it by a symbol. Greek letters and unusual symbols should be identified in the margin. Fractional exponents should be used instead of root signs.

25

EFFECT OF WORLD-WIDE CHANGES OF ISOTROPIC COSMIC RAY INTENSITY ON THE DAILY VARIATION OF COSMIC RAYS

R. P. KANE

PHYSICAL RESEARCH LABORATORY, AHMEDABAD

(*Received, February* 14, 1961)

ABSTRACT. Various methods of evaluating the 12 bi-hourly values required for a study of the daily variation of cosmic ray intensity are discussed. Estimates are obtained of the distortions produced in the genuine daily variation due to slope, curvature and short-term effects of the world-wide fluctuations in isotropic cosmic ray intensity. A method for correcting for such effects is suggested and examined critically.

I. INTRODUCTION

The daily variation of cosmic ray intensity is a very important tool for the study of anisotropy of cosmic rays. Daily variation is usually studied by examining the form of the daily curve as a whole or by resolving the same into its Fourier components. It can be studied for individual days, if the statistical accuracy of the data is good enough, or for averages over groups of days. For data having large statistical errors on individual days, histograms of harmonic components obtained for individual days could still lead to useful conclusions.

However, while studying the daily variation of cosmic ray intensity, allowances are to be made for the effects due to world-wide changes of the isotropic cosmic ray intensity as these are likely to distort the true form of a genuine local-time daily variation. Whereas the possibility of such distortions is recognised by workers in this field, some of the recently published results seem to indicate that the extent of these distortions is not fully appreciated. The purpose of the present communication is to estimate the magnitude of such distortions under various conditions and for various aspects of study of the daily variation.

II. METHODS OF STUDY OF DAILY VARIATION

The basic requirement for a study of the daily variation is the evaluation of hourly or bi-hourly percent deviations from mean. Since most of the workers use bi-hourly deviations, we will henceforth consider only these. Percent bi-hourly deviations are usually obtained by the following methods :—

Method A : Evaluating the arithmetic mean of 12 successive bi-hourly values and expressing each bi-hourly value as percent deviation from this mean.

Method B : Applying correction for the linear gradients of cosmic ray intensity by subtracting the 0 hour value of one day from the 0 hour value of the next day. The difference so obtained is expressed as percentage of the day's mean. If this percentage value is designated as d, one subtracts the factor $\left(\frac{n-6.5}{12}\right)\times d$ from the nth bi-hourly deviation obtained by method A above.

Method C : Applying correction for the linear gradients by evaluating moving averages of 12 successive bi-hourly values and subtracting these from the original bi-hourly values. Since a mean of 12 successive values has an hour of centering not coincident with any bi-hourly value but lying half-way between two bi-hourly values, two alternatives are usually adopted :

(i) Moving averages of 12 bi-hourly values are further subjected to moving averages over 2 consecutive values so that the new means so obtained have centering coincident with the original bi-hourly intervals.

(ii) Moving averages are calculated for 13 successive bi-hourly values instead of 12 sucessive values so that the centering is the same as for original bi-hourly values.

In principle, procedure (ii) is less rigorous; because moving averages over 13 consecutive bi-hourly values leave some residual daily variation in the means. In practice, both methods give almost similar results.

Fig. 1 is an illustration of the three methods and the daily variations obtained by using them for a sample bi-hourly data for the neutron monitor at Sulphur Mountain for September 21—25, 1957, when the cosmic ray intensity undergoes a depression of about 10% in 2 days and then recovers to almost its original values in the next 2 days. The dotted line at the top (Curve X) is the plot of original bi-hourly values while the full curve Y superimposed on it is the plot of moving averages over 12 consecutive bi-hourly values. Curves A, B, C show the daily variations obtained by methods A, B and C respectively.

The following characteristics will be noticed from Fig. 1 :

(a) The daily variation obtained by method A is not corrected for linear gradients of the cosmic ray intensity and hence bi-hourly percent deviations for the 1st day (September 22, 1957) are positive for the first half of the day and negative for the latter half, creating a false impression of an early morning maximum of the daily variation. For the second

day, the daily variation is characterised by a minimum which is coincident with the point of inflection in the general trend of intensity change. On the third day, the pattern is reverse to that of first day, creating a false impression of afternoon maximum.

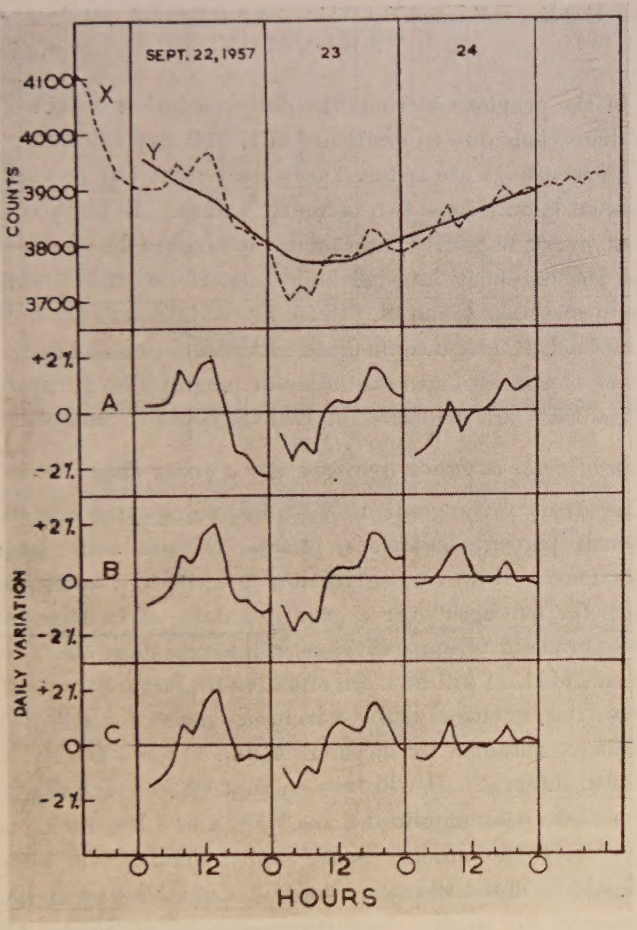

Fig. 1. Bi-hourly values and daily variation for neutron intensity at Sulphur Mountain for September 21–25, 1957.

(b) The daily variation obtained by method B is comparatively free from effects due to gradients on the 1st and 3rd day. However, for the 2nd day, the correction factor has been almost zero as the cosmic ray intensity has gone down and recovered again and the 0 hour values at the beginning of the second and third day are almost the same. Hence the daily variation on the second day is the same as the daily variation for second day obtained by method A.

(c) The daily variation obtained by method C is less affected by effects due to gradients as compared to the daily variations obtained by methods A and B.

III. COMPARISON OF METHODS *A* AND *C* FOR THE STUDY OF VARIOUS ASPECTS OF DAILY VARIATION

As seen in the previous section, the daily variation obtained by method A is subject to distortions due to gradients in cosmic ray intensity. If method B is employed, these effects are reduced to some extent but not fully, because the gradient is evaluated only from two bi-hourly values. In method C, the gradient is estimated at every bi-hourly interval by averaging 12 consecutive bi-hourly values around the bi-hourly interval under consideration. Method C is, therefore, superior to methods A and B. Since methods A and C are at the two extremes and method B has intermediate characteristics, we will consider only methods A and C and estimate the order of magnitude of distortions involved when linear gradients are neglected in various types of analysis.

(1) *Study of daily variation averaged over a group days*

The effect of the gradients is to introduce extra contributions in the bi-hourly percent deviations. Larger the gradients, larger will be the distortions. However, gradients are both positive and negative. Hence for averages over a group of days, it is expected that effects due to gradient of opposite signs will cancel each other to some extent. The cancellation will be more effective for larger groups of days. Fig. 2 shows the average daily variation curves for the neutron monitor at Climax obtained by methods A and C for a 20-day interval and a 6-month interval. It will be seen that whereas for the 20-day interval the peak-to-peak amplitudes are 1.5% and 1.3% for methods A and C respectively, the amplitudes are almost equal for the 6-monthly period. It should be noted that the amplitudes obtained by method A need not necessarily be larger. Distortions due to gradients will enhance or reduce the amplitudes depending upon whether the phase of the extra contribution is similar or opposite to the phase of the genuine variation.

(2) *Study of the frequency distributions of the amplitudes and time of maxima of the diurnal and the semi-diurnal components of the daily variation.*

A useful way of studying the daily variation is by resolving the 12 bi-hourly percent deviations into Fourier (harmonic) components for every day and studying the frequency distributions of the amplitudes and time of maxima. However, such frequency distributions will suffer distortions if the general level of cosmic ray intensity is increasing

or decreasing with constant gradients. The effects of linear gradienst can be estimated by subjecting to harmonic analysis idealised bi-hourly deviations giving straight line plots. Table I below gives such estimates for the amplitudes and time of maxima of the 1st and 2nd harmonics for positive and negative linear gradients of 1.0% over 24 hours.

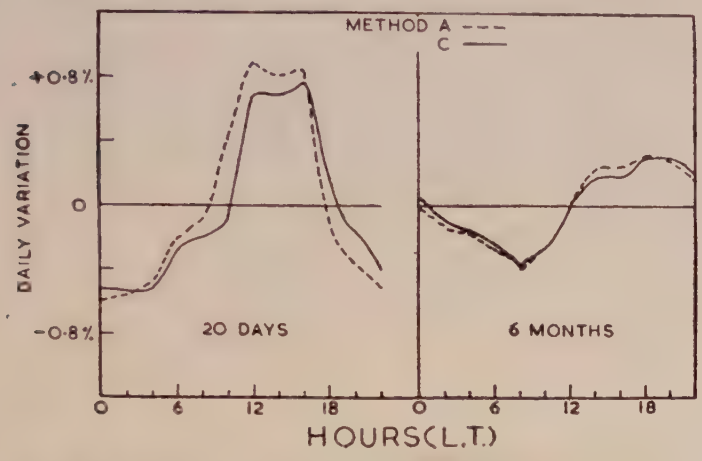

Fig. 2. Average daily variation for neutron intensity at Climax for a 20-day and a 6-month period.

TABLE I

	Amplitude r_1	Time of max. ϕ_1	Amplitude r_2	Time of max. ϕ_2
Linear increase of 1.0%/24 hours.	0.32%	$\pi+75°$	0.17%	$\pi+60°$
Linear decrease of 1.0%/24 hours.	0.32%	75°	0.17%	60°

In practice, these vectors will be superimposed upon the genuine diurnal and semi-diurnal vectors.

To see how these distortions occur in actual data, the bi-hourly values of neutron intensity at Climax were treated by methods A and C and harmonically analysed for individual days for a 12 month period. Fig. 3 shows the frequency distributions for the amplitudes (r_1 and r_2) and the time of maxima (ϕ_1 and ϕ_2) of the first and second harmonics respectively obtained by methods A and C. It will be noted that the amplitudes of the first harmonic extend to larger values in method A. Also the frequency distribution of the time of maximum ϕ_1 of the first harmonic has a larger spread in method A.

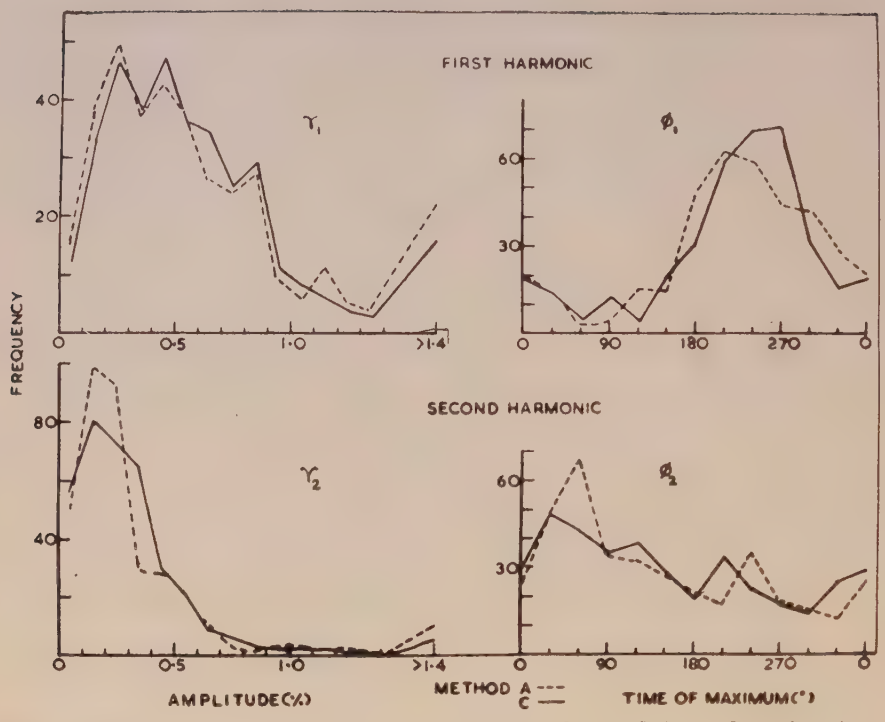

Fig. 3. Frequency distributions for the amplitudes (r_1 and r_2) and times of maxima (ϕ_1 and ϕ_2) for the first and second harmonics for Climax neutrons.

(3) *Relationship between daily variation and daily mean intensity.*

For studying a relationship of this type, it is obvious that method A is not suitable; because the daily variation is already distorted by gradients in daily mean intensity to the extent indicated in Table I.

(4) *Solar and Terrestrial relationships of daily variation*

It is well known that the daily mean intensity of comic rays is related to geomagnetic disturbances as well as some solar phenomena. If, therefore, the daily variation of cosmic rays is studied by method A, all such relationships will affect the characteristics of the daily variation also. Therefore, for this type of analysis, method A is not suitable.

(5) *Study of individual bi-hourly deviations*

As can be seen from Fig. 1, the individual bi-hourly deviations obtained by method A can be greatly distorted by the general trend in the daily mean intensity. Hence, method A is not suitable for this type of study.

It may be concluded, therefore, that except for periods when the fluctuations in the daily mean intensity are small compared to the expected amplitudes of

daily variations or except when daily variations averaged over long periods are under consideration, the use of method A is undesirable for a study of the daily variation, as it is distorted by what may be termed as "Slope effects". Method B is better than method A but has its limitations as already referred to above. Method C is more rigorous and has a smaller Poisson standard error and hence is preferable to methods A and B for most purposes.

IV. A CRITICAL APPRAISAL OF METHOD *C*

It was shown in the previous section that amongst the three methods for obtaining the bi-hourly percent deviations from mean, method C is the best. However, it is necessary to examine whether method C is completely free from effects due to gradients.

The bi-hourly cosmic ray intensity $I'(t)$ observed at $U.T.(t)$ may be expressed as

$$I'(t) = I(t) + f(T, t)$$
$$= I(t) + \sum_n r_n \sin\{n(t+\psi)+\phi_n\} \quad \ldots \quad (1)$$

where $I(t)$ is the isotropic level of world-wide cosmic ray intensity and $f(T, t)$ is the daily variation, which can be resolved into Fourier components. Since all harmonics of periodicities of 24 hours or fractions thereof, reduce to zero when averages over 24 hours are taken, averages of $I'(t)$ over 12 successive bi-hourly values will be equal to similar averages of $I(t)$. In method C, it is assumed that such averages of $I'(t)$ values for 12 sucessive bi-hourly intervals are good estimates of the instantaneous values of $I(t)$ for the middle of the interval. Such an assumption is valid only when $I(t)$ changes occur with constant gradients. If the gradients (i.e. slopes) change, distortions will be produced which will be roughly proportional to the second derivative d^2I/dt^2 of the (I vs. t) plot. It is obvious, therefore, that method C will give incorrect results during periods when the gradients dI/dt undergo large changes.

The distortions produced due to changes in gradients can be broadly classified into 2 types:

(i) Long-term changes of world-wide cosmic ray intensity with time constant exceeding 24 hours. These will produce distortions which will be termed as "Curvature effects".

(ii) Short-term (hours-to-hour) fluctuations of a world-wide nature in the cosmic ray intensity. These will be termed as "Short-term effects".

The contribution of "Curvature effects" to the daily variation can be estimated if the pattern of the intensity change is known. Consider, for example, the patterns A and B shown in Fig. 4, which represent linear gradient schanging signs abruptly. In Fig. 4, pattern A corresponds to a constant gradient of

+0.1%/hr. for 18 successive bi-hourly values, followed by a sudden change to a constant gradient of −0.1%/hr, for the next 18 bi-hourly values. This pattern corresponds to a change of about 2.4% per day which is not uncommon for cosmic ray neutron intensity at high latitudes. Pattern B corresponds to a form exactly opposite to pattern A.

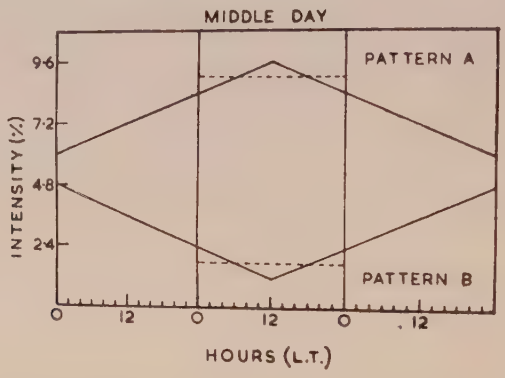

Fig. 4. Sample patterns of sudden changes in the linear gradients of cosmic ray intensity.

If the point of inflection is assumed to coincide with 12 noon (L.T) for the middle day and the data are treated by method C and the bi-hourly percent deviations harmonically analysed, the amplitudes and time of maxima of the first and second harmonics for the middle day are as given in Table II.

TABLE II

	1st harmonic		2nd harmonic	
	Amp.	Time of max.	Amp.	Time of max.
Pattern A	0.24%	180°	0.08%	0°
Pattern B	0.24%	0°	0.08%	0°

It will be seen that amplitudes of the order of 1/4% can arise due to "Curvature effects" on individual days, if the day includes the inflection point. For other days, as also for averages over groups of days, the contribution due to "Curvature effects" will be negligible.

As regards the contribution of "Short-term effects" to daily variation, it is difficult to investigate patterns as there are innumerable ways in which individual bi-hourly values can be affected by world-wide short-term fluctuations of isotropic cosmic ray intensity. From the data from a single station it is impossible to estimate the contribution of such changes to individual bi-hourly values.

V. AN EFFECTIVE METHOD OF ESTIMATING THE WORLD-WIDE SHORT-TERM CHANGES OF COSMIC RAY INTENSITY

As seen in previous section, data from a single station are inadequate to separate out the genuine daily variation of cosmic ray intensity from its experimentally obtained form distorted by possible "Short-term and Curvature effects". For long-term averages, such effects are expected to even out; but for averages over only a few days, there is a possibility of distortions. Unfortunately, it is not possible to estimate their magnitude from the data of a single station.

A little consideration shows, however, that there is a possibility of such an estimate if data from more than one station are utilised. This is already pointed out by Sekido *et al.* (1952). Referring back to Eq. (1), let us assume that cosmic ray data are available for a number of stations which are at the same geomagnetic latitude and are at equally spaced longitudes all round the globe. Then, the cosmic ray intensity $I'_k(t)$ at the k-th station at time (t) would be given by

$$I'_k(t) = I(t) + \sum_n r_n \sin \{n(t+\psi_k)+\phi_n\} \quad \ldots \quad (2)$$

where r_n and ϕ_n represent the amplitude and phase of the nth harmonic for a station of longitude zero ($\psi_0 = 0$) and ψ_k is the longitude of the kth station. If values of ψ_k for successive stations differ by a constant quantity $360/m$, where m is the number of stations, then

$$\psi_k = (k-1)\ \frac{360}{m} \quad \ldots \quad (3)$$

and

$$\sum_{k=1}^{m} r_n \sin \left[n \left\{ t + \frac{360(k-1)}{m} \right\} + \phi_n \right] = 0 \quad \ldots \quad (4)$$

for $n \neq \beta m$, where β is a positive integer,

provided that the amplitudes r_n and phases ϕ_n remain constant for more than 24 hours. Thus, if we concentrate our attention only on the first harmonic(n 1), even two stations (m = 2) separated by $360/m$ 180° will ensure that Eq. (4) is satisfied. To eliminate the second harmonic also (n 2), we will need 3 stations, 120° apart in longitude. If data from 3 such stations are available then the average of the percent cosmic ray values at the 3 places for *the same universal time* (t) will be devoid of the first or second harmonic of genuine daily variation.

It is obvious, therefore, that if the world-wide bi-hourly percent mean intensity obtained by adding the percent values at the same U.T. of 3 stations at roughly the same geomagnetic latitude and spaced 120 apart in geographic longitude

is subjected to an analysis of daily variation by method C, one would get an idea of the characteristics of the *apparent* daily variation introduced due to short-term and curvature effects of the world-wide isotropic intensity changes. With this view, data obtained during I.G.Y. were examined to select out suitable groups of stations. A study of the geographical distribution of neutron monitor stations shows that there is a preponderance of stations in the European and American longitudes but a marked scarcity in the Far East. The following factors have also to be kept in mind :

(a) The stations should be at roughly the same geomagnetic latitude to ensure similar cut-off energies.

(b) They should have similar energy responses related to the altitude.

(c) They should have been corrected for barometric effect by the same pressure coefficients (say, $0.72 \pm 0.02\%/mb$. Hg.).

(d) Data for each of them should be fairly continuous for about 12 months to give a large number of common days.

(e) The counting rate at each station should be fairly high (bi-hourly standard error about 0.5%).

(f) They should be $120 \pm 10°$ apart in geographic longitude.

It was found that the following stations could be utilised for analysis:

(1) Lincoln or Climax in Americas.

(2) Gottingen or Weissenau and some others in Europe.

(3) Yakutsk in the Far East.

From the point of view of spacing in geographical longitude, Climax, Gottingen and Yakutsk is a very convenient group. Since Climax is a high altitude station, Lincoln, Gottingen and Yakutsk is perhaps a more appropriate choice. Table III gives the details about the geographical locations and energy responses etc. for the 4 stations.

TABLE III

Station	Geomag. latitude	Geographical longitude	Altitude (meters)	Cut-off energy (BeV)	Mean Fonger energy response (BeV)
Climax	48°	106°W	3400	3.0	9.7
Lincoln	51°	97°W	350	2.6	12.1
Gottingen	52°	10°E	273	2.4	12.1
Yakutsk	51°	129°E	105	2.2	12.1

The bi-hourly values for Climax, Lincoln, Gottingen and Yakutsk were obtained from the Japanese publication "Cosmic Ray Intensity during the

I.G.Y.—No. 1-2″. Values for the same bi-hourly (G.M.T.) intervals were added to yield bi-hourly values of W and W′ series defined as follows :—

$$W = \tfrac{1}{3}(\text{Climax} + \text{Gottingen} + \text{Yakutsk})$$

$$W' = \tfrac{1}{3}(\text{Lincoln} + \text{Gottingen} + \text{Yakutsk})$$

If the pattern of daily variation remains constant for more than 24 hours, the bi-hourly values of W or W' would be devoid of the 1st, 2nd, 4th and 5th harmonics. The 3rd and 6th harmonics will be retained.

The bi-hourly values of W and W' were treated by method C and the percent bi-hourly deviations obtained for the 12 successive bi-hourly intervals centered at 01, 03...23hr. G.M.T. were considered as a U.T. apparent daily variation* which would give a measure of the distortion involved on any particular date. Except for the fact that the 3rd and 6th harmonics are still retained in W or W' and that some discrepancies would creep in, if the genuine daily variation is of a transient type (this is discussed further in Sec. VII), the characteristics of the daily variation exhibited by W or W' would give an estimate of the "Curvature and Short-term effects" that vitiate the genuine daily variation. In the next section, results obtained for the 12 month period July 1957—June 1958 are described.

VI. CHARACTERISTICS OF THE APPARENT DAILY VARIATION DUE TO "CURVATURE AND SHORT-TERM EFFECTS"

(1) *Variance of daily variation* :

A useful criterion for studying the magnitude of daily variation is the variance which we define as

$$V = \sum_{x} (\delta I_x)^2$$

where (δI_x) is the percent deviation from the day's mean for the bi-hour x. V is a gross measure of the daily variation on any particular day without any reference to the phase of the daily variation, and apart from the contribution due to random statistical fluctuations, is a good measure of the average disturbance.

Variances have been calculated for the world-wide isotropic neutron intensities W and W' as also for the neutron intensities at Climax, Gottingen, Lincoln and Yakutsk. The frequency distributions of V for the period July 1957 to June 1958 are shown in Fig. 5. It will be seen that the variance of the apparent daily variation of W or W' is not negligible and there is an indication that a portion of the daily varia-

* Recently, Parsons (year?) has attempted to estimate the U.T. contribution to the monthly average daily variation curves for the experimental data of several high latitude neutron monitor stations.

tion observed on individual days is attributable to curvature and short-term effects.

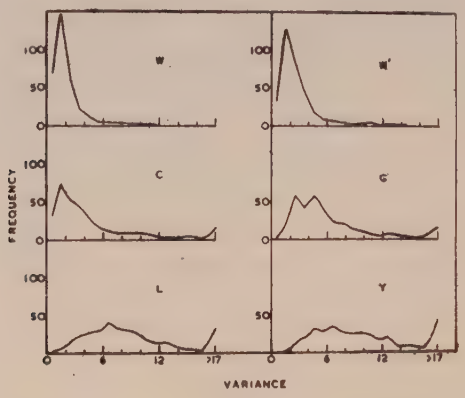

Fig. 5. Frequency distributions of variances for W, W', Climax (C), Lincoln (L), Gottingen (G) and Yakutsk (Y).

(2) *Amplitudes and times of maxima of daily variation* :

A convenient way of studying the daily variation vector is to resolve the 12 bi-hourly values into the first and second harmonics by the usual methods of Fourier analysis. This can be done either for individual days or for averages over a number of days. It would be interesting to see how much of the daily variation on individual days is contributed by short-term and curvature effects. To study this, the percentage bi-hourly deviations for the intensity W and W', treated by method C, were harmonically analysed for every day for which full data were available during July 1957 to June 1958. Fig. 6 shows the frequency distributions for r_1, r_2, ϕ_1 and ϕ_2 i.e., the amplitudes and times of maxima of the first and second harmonics. For comparison, similar distributions for neutron intensity at Climax, Lincoln, Gottingen and Yakutsk for the same period, are shown. It will be noticed that the amplitudes r_1 and r_2 for W and W' are not negligible compared to those for Climax, etc. This confirms our earlier conclusion drawn from the variance distribution that the daily variation on individual days is partly due to short-term and curvature effects as depicted by W and W'. It must be emphasised here that these apparent amplitudes cannot be attributed to random statistical fluctuations. From the known bi-hourly counting rates at the various stations, the Poisson standard errors of the amplitudes on individual days can be calculated. The 2σ levels are indicated in Fig. 6 by vertical dotted lines in the r_1, r_2 frequency distributions. It will also be observed that the distribution of the times of maxima for W and W' shows, as expected, no preference for any particular hours,

while for Climax etc., directions near local noon are favoured most for the first harmonic.

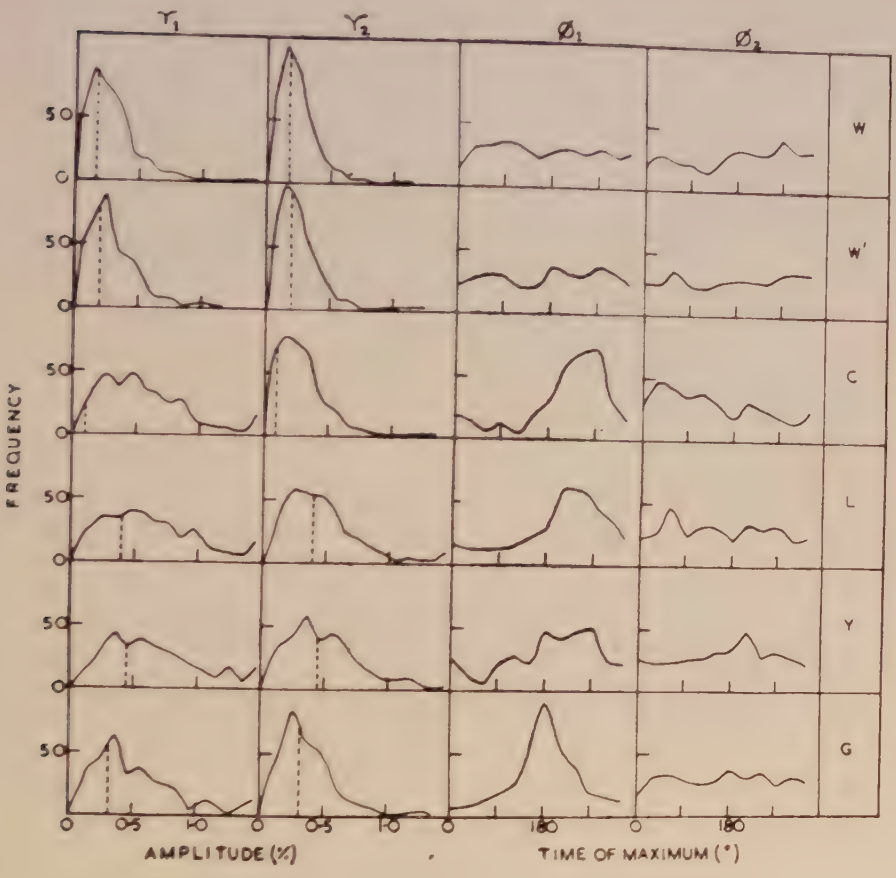

Fig. 6. Frequency distributions for the amplitudes (r_1, r_2) and times of maxima (ϕ_1, ϕ_2) of the first and second harmonics for W, W', Climax, Lincoln, Gottingen and Yakutsk. Vertical dotted lines in r_1, r_2 distributions are 2σ limits.

(3) *Monthly mean daily variation* :

It will be interesting to estimate the contribution of the apparent daily variation when averages over groups of days are considered. Table IV gives the amplitudes and the times of maxima of the 1st and 2nd harmonics of the monthly average daily variations for W, W' and Climax for July 1957 to June 1958. It will be seen that the monthly averages for W and W' are not negligible. The amplitudes for W and W' are about $\frac{1}{3}$rd of those for Climax for individual months but less than 1/5 th for the yearly averages. It is clear, therefore, that the apparent daily variation depicted by W and W' progressively reduces in amplitude

TABLE IV

Month	W				W'				Climax			
	$r_1(\%)$	ϕ_1	$r_2(\%)$	ϕ_2	$r_1(\%)$	ϕ_1	$r_2(\%)$	ϕ_2	$r_1(\%)$	ϕ_1	$r_2(\%)$	ϕ_2
July, 1957	0.12	$\pi+65°$	0.06	$\pi+34°$	0.13	$\pi+94°$	0.08	$\pi-7°$	0.36	$\pi+57°$	0.13	30°
August	0.14	$\pi+21°$	0.09	$\pi+32°$	0.16	$\pi+47°$	0.05	$\pi+53°$	0.49	$\pi+54°$	0.08	68°
September	0.04	135°	0.08	$\pi+50°$	0.03	$\pi+45°$	0.06	$\pi+59°$	0.57	$\pi+32°$	0.13	103°
October	0.02	90°	0.05	$\pi+53°$	0.02	27°	0.06	$\pi+45°$	0.37	$\pi+54°$	0.03	135°
November	0.07	27°	0.08	$\pi+90°$	0.05	+11°	0.08	$\pi+67°$	0.42	$\pi+43°$	0.12	96°
December	0.12	95°	0.02	$\pi+27°$	0.09	117°	0.02	$\pi+90°$	0.09	$\pi+20°$	0.07	21°
January, 1958	0.03	$\pi+71°$	0.03	$\pi-18°$	0.09	144°	0.04	56°	0.34	$\pi+75°$	0.06	15°
February	0.15	53°	0.05	$\pi+37°$	0.06	− 9°	0.07	−34°	0.48	−34°	0.13	156°
March	0.06	$\pi+9°$	0.04	$\pi+27°$	0.09	$\pi+32°$	0.02	$\pi+63°$	0.23	$\pi+76°$	0.07	−7°
April	0.04	−27	0.07	−63°	0.05	−53°	0.05	−79°	0.34	$\pi+72°$	0.05	130°
May	0.03	109°	0.05	−53°	0.06	$\pi+9°$	0.04	−56°	0.29	$\pi+91°$	0.06	139°
June	0.12	104°	0.05	−90°	0.10	151°	0.03	−45°	0.49	−56°	0.09	86°
Yearly average	0.03	108°	0.04	$\pi+63°$	0.03	$\pi+18°$	0.03	$\pi+90°$	0.32	$\pi+69°$	0.06	83°

when averages over large periods (about an year) are obtained. For smaller periods, considerable distortions can occur.

(4) *Contribution of the apparent daily variation to averages over groups of days selected on physical criteria* :

For studying solar and geomagnetic relationships of the daily variation, the usual procedure is to select groups of days according to certain criteria and evaluate the average daily variations. For example, one could compare average daily variations on magnetically disturbed and quiet days. One could attempt to find correlated changes between daily variation and daily mean intensity and so on. Several workers have reported results of these types in the past.

It must be noted, however, that in some of these criteria the days selected are such that they are associated with large gradients and curvatures of cosmic ray intensity. For these, the apparent daily variation due to curvature and short-term effects is expected to be large. A preliminary analysis conducted by us for groups of days selected on the usual geomagnetic criteria has indicated that many of the characteristics reported for daily variation for days conforming to such criteria are shown to some extent by the apparent daily variation also. This does not exclude the possibility that such characteristics will be depicted by genuine daily variation. It needs to be confirmed, however, that such characteristics are still shown when the observed daily variation is corrected for effects due to the apparent daily variation.

It must be pointed out here that the estimates of the apparent daily variation due to short-term and curvature effects as given above are only for middle latitude, neutron monitor intensities. The effects are roughly proportional to the range of fluctuations of cosmic ray intensity. Since the daily mean intensities of neutron component and meson component at equator show fluctuations about $\frac{1}{2}$ and $\frac{1}{3}$ to $\frac{1}{4}$ respectively of the mean intensity fluctuations of neutron intensity at middle latitudes, it would seem that the distortions due to apparent daily variation would be lesser in the above proportions for equatorial neutrons and mesons. This will certainly be true for curvature effects which are of periodicities greater than 24 hours. For short-term fluctuations, it requires to be checked whether hour-to-hour changes of world-wide isotropic intensities have also the same latitude dependence as fluctuations of daily mean intensity.

VII. METHOD OF STUDYING THE GENUINE DAILY VARIATION OF COSMIC RAY INTENSITY

It is clear from the above discussion that the daily variation of cosmic ray intensity can be in error when studied for short periods from the data of only one

station. The results will be distorted due to the presence of an apparent daily variation due to world-wide fluctuations of isotropic intensity. The magnitude of the latter can be estimated by combining data from three or more stations at roughly the same geomagnetic latitude and equally spaced in geographical longitudes. On the other hand, to eliminate the contribution of the apparent daily variation and to study the genuine daily variation of cosmic ray intensity, it would be necessary to subtract the world-wide intensity fluctuations from the original data of any one station. To give a specific example, we have, in the present communication, combined the data from the stations Climax, Gottingen and Yakutsk for similar bi-hourly intervals (U.T.) to obtain the series W. One could now subtract the bi-hourly values of W from the bi-hourly values of Climax, Gottingen or Yakutsk for the same U.T. and obtain series of bi-hourly values which, when considered according to the local time of the particular station, would give the basic 12 bi-hourly values for study of the daily variation. To improve the statistics, one could superimpose the local time bi-hourly values of the three stations. On the other hand, since the daily variation may be of a transient nature, one may prefer to study the data obtained for the three stations individually and observe the 8 hourly changes in the nature of the daily variation. Such an analysis may prove very fruitful for studying the influence of S.C. storms as well as solar flares which are comparatively of short duration.

It is necessary, however, to discuss at this stage the merits and demerits of this method for all aspects of the study of daily variation. The necessity of adopting the present method arises from the existence of short-term and long-term world-wide changes in the mean level of isotropic cosmic ray intensity. Also, its success depends upon its ability to eliminate these changes without eliminating a genuine daily variation. This is achieved if the genuine daily variation is of a constant pattern. In practice, however, one is likely to encounter complex patterns of daily variation. It is necessary to study in detail the various types of effects that one may observe in daily data. Since the basic data are averaged over a bi-hourly interval, we will consider bi-hourly percent deviations as our basic unit. Samples of various cases are illustrated in Fig. 7, where C, G and Y represent bi-hourly values at Climax, Gottingen and Yakutsk respectively, for the same U.T. indicated on abscissa, and W represents the average given by

$$W = \tfrac{1}{3}\,(C+G+Y)$$

(i) Climax, Gottingen and Yakutsk all show a positive (or negative) bi-hourly deviation of the same magnitude at a particular bi-hourly interval. Then W will also show a similar deviation at the same hour. This is illustrated in Fig. 7(i) and is a true world-wide effect with magnitudes remaining the *same* for C, G, Y, as also for W.

(ii) Climax shows a bi-hourly deviation at a particular hour U.T. and Gottingen and Yakutsk show the same deviation but 8 and 16 hours

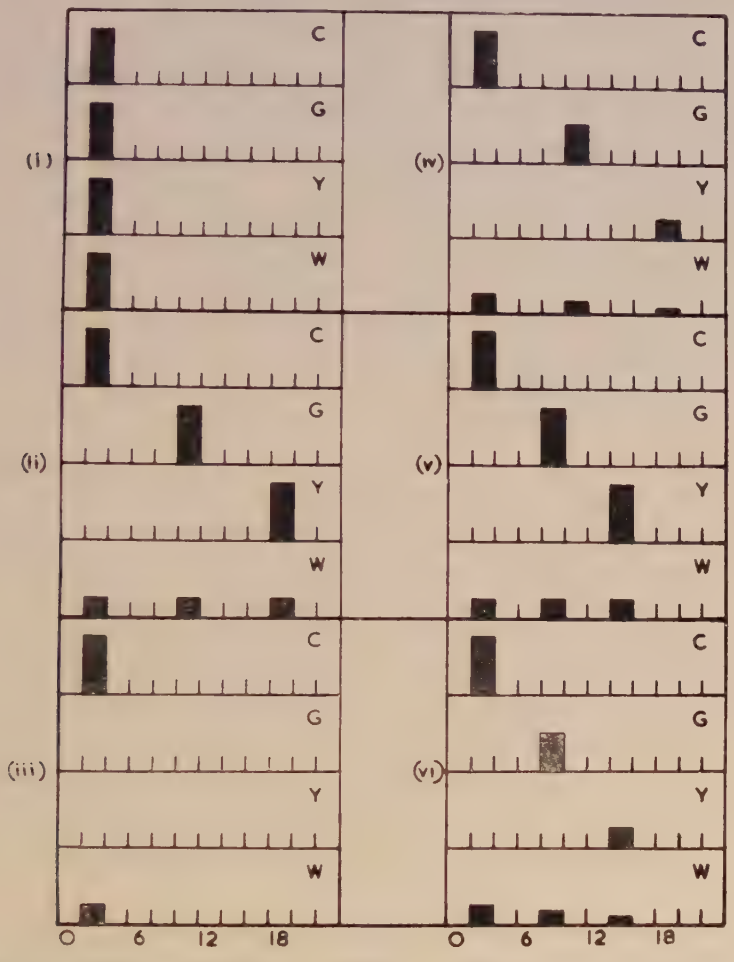

Fig. 7. Sample patterns of bi-hourly deviations for Climax (*C*), Gottingen (*G*), Yakutsk (*Y*) and their average (*W*).

later respectively. This is a genuine L.T. daily variation effect. It is illustrated in Fig. 7 (ii) and its effect on *W* will be to produce three humps 8 hours apart and 1/3rd in size. If harmonically analysed, the *W* curve for such a day will show an absence of 1st, 2nd, 4th and 5th harmonic. The 3rd and 6th harmonics will be present.

(iii) Climax shows a bi-hourly deviation at a particular hour U.T. but Gottingen and Yakutsk do not show any effect at this hour or 8 and 16 hours later. This is an impact zone type effect where Climax was in a location suitable for observing the effect but Gottingen and

Yakutsk were not. This is illustrated in Fig. 7 (iii) and produces a deviation in W of magnitude about 1/3rd of that at Climax. This could as well occur at Gottingen or Yakutsk and in each case, W curve will be biased towards that station.

It should also be noted that for individual bi-hourly values, such an impact zone effect cannot be distinguished from high positive or negative deviations occurring at different stations at certain hours due to instrumental troubles unless data from stations in about the same geographical region and altitude are available for comparison.

(iv) Climax shows a bi-hourly deviation at a particular hour U.T. and Gottingen and Yakutsk show reduced or negligible amplitudes 8 and 16 hours later. This is a genuine daily variation, the amplitude of which is changing rapidly, during the course of a few hours [Fig. 7 (iv)]. In this case, the various harmonics will not cancel out in the average curve W. In fact, W will show roughly the same type of variation as in (iii) above.

(v) Climax shows a bi-hourly deviation at a particular hour U.T. and Gottingen and Yakutsk show the same amplitudes but not 8 and 16 hours later, but somewhat earlier [Fig. 7(v)]. This is a case where a genuine daily variation is constant in amplitude but has a *changing phase.* Here again, the daily variation will not cancel out in W but will leave a residual variation of about 1/3rd amplitude. In extreme cases where phase shifts are very large, the effect in W could be comparable in magnitude to that at Climax or Gottingen or Yakutsk.

(vi) One could imagine cases where both the amplitudes and phases change rapidly in the course of a few hours as in Fig. 7(vi). Here again the maximum amplitude in W would be lesser than the maximum disturbance among the three stations.

If now an attempt is made to study the genuine daily variation by subtracting W curve from the C, G and Y curves and considering $(C-W)$, $(G-W)$ and $(Y-W)$ as representative of the *genuine* daily variations for Climax, Gottingen and Yakutsk respectively, the following will happen :

(i) The genuine daily variation so obtained will be completely free from any distortion effects due to *world-wide* changes of cosmic ray intensity. This will be true for individual bi-hourly values and hence for all the harmonics of a daily variation.

(ii) If the daily variation is constant in amplitude and phase for more than 24 hours, this method will give correct results for the 1st, 2nd, 4th and 5th harmonics. The 3rd and 6th harmonics will, however, be missing. For individual bi-hourly deviations, this method will show such deviations reduced to about 2/3rd of their original values.

(iii) If the genuine daily variation is of a rapidly changing pattern the effect of the present method will be again to reduce the amplitudes to about 2/3rd of their original values. This will roughly be true for bi-hourly deviations as also for the various harmonics. In the case of the latter distortions in phases would also be expected.

(iv) All abnormalities like impact zone effects or bi-hourly deviations due to faulty data will be reduced to about 2/3rd of their original values.

Therefore, while taking a decision as to whether one should study daily variation of cosmic ray intensity by the present method or by the usual method C adopted for individual stations, one has to choose between two alternatives viz., to eliminate world-wide short-time fluctuations of cosmic ray intensity but in the process to reduce the amplitudes of the *rapidly changing portion* of daily variation to about 2/3rd of its original amplitude or, to retain fully all genuine daily variation but allow distortions due to world-wide short term fluctuations of isotropic intensity. Such a decision would largely depend upon the relative magnitudes of the genuine daily variation and the apparent daily variation produced by short-term world-wide fluctuations. It would be worthwhile getting an estimate as to how often world-wide short term fluctuations occur in a given data. For this purpose the data for W as described in the present paper were considered as follows:

Since the Poisson bi-hourly standard errors of Climax, Gottingen, Yakutsk and W are 0.12%, 0.41%, 0.56% and 0.24% respectively, amplitudes of about 0.3%, and 0.5% or more are significant on a 2σ level (95% correct) for Climax and W respectively, but not for Gottingen and Yakutsk. However since the standard error of *Gottingen plus Yakutsk* is about 0.69%, a value of 1.4% or more for this sum would be significant on a 2σ level. Hence days were selected on which at least one bi-hourly deviation for W exceeded 0.5% numerically. Such days were termed as disturbed days. Now W is related to Climax, Gottingen and Yakutsk as

$$W = \tfrac{1}{3}(C - G - Y).$$

Therefore, it was further examined whether a particular large bi-hourly deviation of W was largely due to C (Climax) or due to Gottingen and/or Yakutsk or due to all the three. The following categories were obtained:

Category (a): (W due to world-wide isotropic change.)	For positive W values. (i) $W \geqslant +0.5\%$ (ii) $C \geqslant -0.3\%$ (iii) $(3W-C) > -1.4\%$	For negative W values. (i) $W \leqslant -0.5\%$ (ii) $C \leqslant -0.3\%$ (iii) $(3W-C) < -1.4\%$
Category (b): (W attributable to Climax only)	For positive W values. (i) $W \geqslant +0.5\%$ (ii) $C \geqslant +0.3\%$ (iii) $(3W-C) < +1.4\%$	For positive W values. (i) $W \leqslant -0.5\%$ (ii) $C \leqslant -0.3\%$ (iii) $(3W-C) > -1.4\%$
Category (c): (W due to Gottingen and/or Yakutsk only)	For positive W values. (i) $W \geqslant +0.5\%$ (ii) $C < +0.3\%$	For negative W values. (i) $W \leqslant -0.5\%$ (ii) $C > -0.3\%$

On actually separating out the experimental data by the above criteria, the following statistics were obtained:

Total No. of days for which data were available	318
Total No. of days on which not a single bi-hourly for W exceeded 0.5% numerically (Quiet days)	61
No. of disturbed days	257
No. of days of Category (a) (W world-wide)	121
No. of days of Category (b) (W Climax-dominated)	94
No of days of Category (c) (W dominated by Gottingen or Yakutsk) ...	178

It is obvious, however, that many days are common to the three categories (a), (b) and (c). A further breakdown was therefore attempted and yielded the following results :

Total No. of disturbed days.		257
Category A :	Days on which one or more bi-hourly deviations of W were due to all the three stations (exclusive world-wide effect)	39
Category B :	Days on which one or more bi-hourly deviations of W could be attributed to Climax *exclusively*.... ...	28
Category C :	Days on which one or more bi-hourly deviation of W could be attributed *exclusively* to Gottingen and/or Yakutsk.	80
Category D :	Days on which some bi-hourly deviations were due to Climax and some due to world-wide effect. (a)+(b) category.	12
Category E :	Days on which some bi-hourly deviations were due to Climax and some due to Gottingen and/or Yakutsk. (b)+(c) category.	28
Category F :	Days on which some bi-hourly deviations were due to world-wide effect and some due to Gottingen and/or Yakutsk. (a)+(c) category.	44
Category G :	Days on which some bi-hourly deviotions were due to Climax, some due to world-wide effect and some due to Gottingen and/or Yakutsk. (a))+(b)+(c) category.	26
	Total (A+.....G)	257

It seems, therefore, that almost all types of variations are present in the data in various degrees. Thus, categories B. C and E are solely due to fluctuations at Climax, or Gottingen or Yakutsk. Due to lack of statistical accuracy, it is impossible to judge which of these are due to genuine daily variation of constant pattern and which are due to genuine daily variation of rapidly changing pattern. Also, all impact zone effects as well as abnormal fluctuations due to faulty data

would be included here! Category A represents days *exclusively* of the world-wide type while categories D, F and G are of a world-wide as well as individual type, category G having the utmost disturbance.

The effect of each one of these categories on the results of daily variation studied by the present method is already discussed above. It would be interesting to see what is the contribution of these to the amplitudes of the first harmonic of daily variation of W. Since frequency distribution for a few days would not be very meaningful nor are the categories completely unambiguous, the various categories referred to above were grouped as follows :

Group 1...Category B, C, E ... Days 136
Group 2...Category A, D, F, G ... Days 121

Fig. 8 shows the frequency distribution of r_1, the first harmonic of the daily variation of W for the two groups. It will be seen that the amplitudes of Group 1 which contains effects on W of L.T. variations at all the three stations as also impact zone and faulty data effects, are confined to lower magnitudes than the amplitudes of Group 2 which represents world-wide fluctuations.

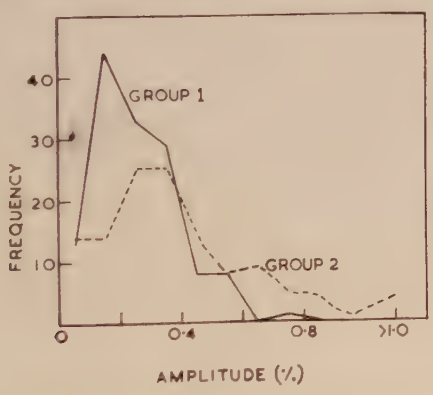

Fig. 8. Frequency distribution of the amplitude of first harmonic (r_1) of W for Groups 1 and 2.

It would seem, therefore, that on almost half the number of disturbed days (121 in 257), the large values of W are either fully or partly due to world-wide effects which can produce apparent amplitudes as large as 0.5% for the first harmonic of daily variation. It would hardly be necessary to emphasise the necessity of correcting for this effect by subtracting W from the individual stations. On the other hand, such a procedure would reduce the amplitudes of the changing type of daily variation for 218 days (Categories B, C, D ,E, F, G) to about 2/3rd of their original values. For many of these days, the amplitudes will be due to instrumental faults, because as shown in an earlier publication (Kane, 1960), many of the I.G.Y. neutron monitor stations have discrepancies of the order of 1—2% in their bi-hourly values. Also, there will be no reduction in amplitude or

distortions of phase for the 1st, 2nd, 5th and 6th harmonics if the genuine daily variation has not changed its pattern radically during the course of a day. The reduction will be only for genuine daily variation patterns which change rapidly within a few hours. Due to statistical uncertainties, it is impossible to estimate the number of days on which only such patterns existed.

The choice is, therefore, between allowing apparent daily variations of amplitudes as high as 0.5% to distort the genuine daily variation or to eliminate the apparent variation and in this process, reduce the amplitudes of genuine daily variations of rapidly changing patterns to about 2/3rd their original value. The present author feels that the latter would be the lesser evil. The reduction effect given by $\left(1-\frac{1}{m}\right)$ when m = Number of stations could be greatly minimised if data from more than three stations equally spaced in geographic longitude and confined to roughly the same geomagnetic latitude were available for analysis. Unfortunately, in the grid of I.G.Y. neutron monitor stations, it is difficult to pick out even groups of three equally spaced stations. The best one can do is to concentrate on groups like Climax (or Lincoln), Gottingen, Yakutsk and to study the daily variation after subtracting from each one of these the corresponding W curve. Work in this direction is in progress.

VIII. CONCLUSION

The results of the present analysis may be summarised as follows :

(1) Except for studying averages over very long periods (about an year), it is necessary to apply corrections for the slope, curvature and short term effects due to world-wide fluctuations of mean cosmic ray intensity.

(2) The slope effects can be effectively corrected for by assuming linear changes as done in method B or method C. The curvature effects are difficult to correct but are fortunately of a small magnitude ($\sim$0.2%). The short-term world-wide effects are the most important ones, on occasions, as large as 0.5% for neutrons at middle latitudes, and cannot be corrected for unless data from stations in the same geomagnetic latitude belt and equally spaced in geographic longitude are available.

(3) For studying only the first harmonic of daily variation, two stations 180° apart are adequate. If, however, higher harmonics are to be considered, the number of stations should be at least three. In view of the several complicated patterns of daily variation which are known to exist, the larger the number of stations, the better. Unfortunately, the present distribution of neutron monitor stations in the world is not quite adequate for this purpose. Attention is drawn of active workers

in this field to the gaps in the longitudinal distribution of cosmic ray recording instruments.

(4) An analysis of data from Climax, Gottingen and Yakutsk indicates that the curve W obtained as an average of these three, exhibits an apparent daily variation having some characteristics similar to those reported as belonging to the genuine daily variation of cosmic ray intensity. It seems necessary to correct for the apparent daily variation produced due to world-wide fluctuations of isotropic cosmic ray intensity.

(5) The magnitude of the distortions is directly proportional to the fluctuations of isotropic intensity. Fluctuations of daily mean intensity are roughly in the proportion 1 : 2 for equatorial and high latitude neutron intensities. Therefore, distortions due to slope and curvature effects would be about half at equatorial stations. For meson intensity the effects would be still less. It is not known, however, whether the short-term (hour-to-hour) fluctuations have the same latitude dependence as the daily mean intensities. This needs further scrutiny.

ACKNOWLEDGMENTS

The author is grateful to Prof. V. A. Sarabhai for helpful discussions. Thanks are due to Miss Kundabala and others for computational assistance and to the Atomic Energy Commission of India for financial assistance.

REFERENCES

Kane, R. P., 1960, *Proc. Ind. Acad. Sc.*, **52***A*, 69.

Sekido, Y., Yoshida, S. and Kamiya, Y., 1952, *Rep. Ionos. Res. Japan*, **6**, 195.

Parsons, N. R., "Phase changes in the daily variation of the cosmic ray nucleonic component" (under publication).

26

F^{19} NUCLEAR MAGNETIC RESONANCE IN POLYCRYSTALLINE MgF_2

S. K. GHOSH, J. LAHIRI AND S. K. SINHA

SAHA INSTITUTE OF NUCLEAR PHYSICS, CALCUTTA

(*Received, February* 21, 1961)

ABSTRACT. Fluorine (F^{19}) nuclear magnetic resonance line shape has been recorded in polycrystalline MgF_2. The second moment of the recorded line-shape has been compared with that computed from the known lattice structure of MgF_2 crystal as given by X-ray diffraction studies. The agreement is satisfactory.

I. INTRODUCTION

The nuclear magnetic resonance (N.M.R.) lines in solid substances are generally broad, and very often show fine structures (Pake, 1948; Gutowsky *et al.*, 1949). Though the prominent fine-structures observed in single crystals are considerably obliterated in polycrystalline samples, the line-shape study in polycrystalline samples can yield significant informations regarding the lattice structures of the crystals concerned (Andrew, 1955).

In general, the energy levels available to a system of nuclear spins placed in a steady external magnetic field $\boldsymbol{H}_0$, are sharp when there is no mutual interactions between the nuclear spins. In such cases the absorption lines observed in the usual N.M.R. experiments are also sharp. When the mutual interactions are present, the discrete energy levels described above are spread almost into a continuum, and the populations of these energy levels are mainly determined by the spatial configuration of the nuclear spins in the system. As a result the absorption lines become broad, and their shapes reflect the above spatial arrangement. Thus, in principle, one can test a suggested spatial arrangement of nuclear spins (for example, the lattice structure of a crystal) by computing the expected line-shape with known forms of the mutual interactions between the spins, and comparing it with the observed line-shape in N.M.R. experiments. It is, however, seen (Broer, 1943) that even if only the magnetic dipole interactions between the nuclear spins are considered, the rigorous derivation of the complete line-shape becomes prohibitingly complicated when the effective number of the interacting spins is large. In such general cases (distinct from the systems containing strongly interacting pairs) the first and the second moments of the line shape function can be computed easily (Van Vleck, 1948; Pake *et al.*, 1948) and can be compared with that obtained from the experimentally recorded line shape. This method of second moment has been shown (McCall and Hamming, 1959)

to be capable of leading one to establish the correct lattice structure in a single crystal, where one has to start from a plausible structure and change the lattice parameters in a systematic way to fit the observed second moments recorded with different crystal orientations with respect to the external magnetic field.

However, in powdered crystals such studies are obviously not possible. Here the expression for the second moment is to be suitably averaged over all orientations of the crystals with respect to the external magnetic field, and one observes only this averaged second moment. This again can be computed on the basis of a suggested crystal structure and compared with the observed value. Such comparison is quite an efficient method of checking that suggested lattice structure, especially when only the magnetic dipole interaction is predominant.

The present report describes the study of F^{19} resonance in MgF_2 powder by the steady N.M.R. method, and a comparison of the second moment thus observed with the value computed from the lattice structure of MgF_2 crystals as given by X-ray diffraction. The agreement is fairly good. In Section II, the results obtained for MgF_2 power are presented and discussed.

II. F^{19} N.M.R. LINE SHAPE IN MgF_2 POWDER

The steady line shape was recorded in a Varian NMR Spectrometer (V4200B) with the Varian electromagnet system (V2100A). A G-10 recorder was used to record the derivative of the F^{19} absorption signal. The precision field scanning dial was calibrated by observing the rotation of the dial required to bring back a proton signal (from H_20) when the *rf* was shifted by a known amount. This change in *rf* was measured by a beat method with the help of a standard frequency generator (HP200D) in conjunction with a harmonic generator.

The sample was polycrystalline MgF_2 (B.D.H. analar grade), sealed in a Pyrex glass tube.

The F^{19} signal was observed at two different settings of the spectrometer. In both of them the *rf* amplitude, the sweep amplitude and the field scanning rate were kept low enough to avoid extra broadening and distortion of the line. In one set (*rf*~6.6 Mc/sec), the values of the above quantities were ~20 m. gauss, ~0.5 gauss, and ~6 m. gauss sec. respectively; and in the other (*rf*~10.7 Mc/sec), they were ~30 m. gauss, ~0.5 gauss and ~11 m. gauss/sec. respectively. Fig. 1 shows one of these recorded derivative curves.

Experiments were carried out at room temperature (80°F).

The second moment, $<\Delta H^2>_{av}$ has been calculated directly from the derivative curves by using the formula

$$<\Delta H^2>_{av} = \frac{1}{3}\left[\int_{-\infty}^{+\infty} (\Delta H)^3 \frac{dg(\Delta H)}{d(\Delta H)}\, d(\Delta H)\right] \Big/ \left[\int_{-\infty}^{+\infty} (\Delta H) \frac{dg(\Delta H)}{d(\Delta H)}\, d(\Delta H)\right] \quad (1)$$

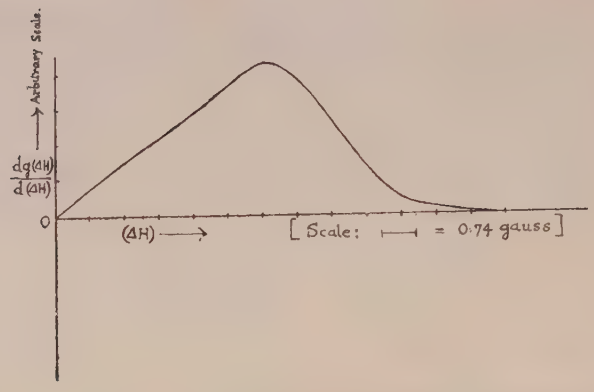

Fig. 1. Derivative of F^{19} N.M.R. absorption signal from MgF_2 powder.

where $\Delta H = H^* - H$, H^* being the resonance value of the magnetic field, corresponding to the centre of the line, and $g(\Delta H)$ is the amplitude of the absorption signal. The average value from nine independently recorded derivative curves (made symmetric by graphical method) has been considered. This value together with the value computed from the lattice structure as given by X-ray diffraction studies (Baur, 1956) is shown in Table I. The X-ray diffraction method shows that a unit cell in MgF_2 crystal can be drawn as shown in Fig (2), with the following values for the lattice parameters :

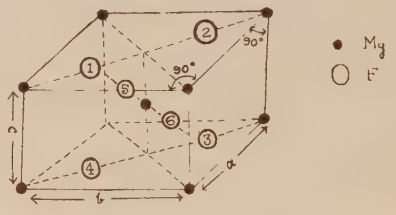

Fig. 2. Unit cell of MgF_2 crystal (X-ray diffraction).

$$a = b = 4.625 \pm 0.002 \text{ Å}$$

$$c = 3.052 \pm 0.03 \text{ Å}$$

and the distances of the fluorine atoms from the central magnesium atom are

$Mg-F(N) = 1.997 \pm 0.005$ Å, for $N = 1, 2, 3, 4$

and $Mg-F(N) = 1.982 \pm 0.007$ Å, for $N = 5, 6$

a, b, and c are perpendicular to each other.

For computation of the second moment from the above lattice structure the following formula (Van Vleck, 1948) has been used,

$$<\Delta H^2>_{av} = 316.9148(1/m) \sum_{j}^{1,..,m} \sum_{k}^{1,..,N} r_{jk} + 6.960(1/m) \sum_{k}^{1,..,m} \sum_{f}^{1,..,N} r_{kf} \quad \ldots \quad (2)$$

Here 'm' is the number of fluorine atoms in the group that repeats itself throughout the crystal, and N is the total number of fluorine atoms in the sample. r(Å) is the radial distance between two nuclei, and 'j', 'k' refer to fluorine nuclei whereas 'f' refers to magnesium nuclei. As is seen from the relation (2), only the magnetic dipole interaction between the nuclear spins has been considered, and the lattice has been assumed rigid. The "exchange interaction" (Bloembergen and Rowland, 1955) between Mg^{25} and F^{19} has not been considered since its contribution to the second moment is expected to be very small. The second term in Eq. (2) has also not been computed since the natural abundance of Mg^{25} is only 10.05% and its magnetic moment is also small compared to that of F^{19}. In computing second moment from Eq.(2), only the nearest neighbours at distances less than 10 Å have been taken into account. The neighbours further apart will add only a negligibly small contribution.

TABLE I

Second moment $<\Delta H^2>_{av}$ of F^{19} resonance line from MgF_2 powder

	$<\Delta H^2>_{av}$ in gauss^2
Computed from given lattice structure	8.54
From the recorded N.M.R. line shape	8.5 $\pm$0.5

As seen in Table I, the agreement between the observed and the computed second moments is quite satisfactory.

ACKNOWLEDGMENT

The authors are thankful to Professor A. K. Saha for kindly going through the manuscript, and for his interest in the work. They are also thankful to Mrs. T. Roy for many of her critical comments.

REFERENCES

Andrew, E. R., 1955, "Nuclear Magnetic Resonance", Chapter 6, The University Press, Cambridge.

Baur, W. H., 1956, *Acta Cryst.*, **9**, 515.

Bloembergen, N. and Rowland, T. J., 1955, *Phys. Rev.*, **97**, 1679.

Broer, L. J. F., 1943, *Physica*, **10**, 801.

Gutowsky, H. S., Kistiakowsky, G. B., Pake, G. E. and Purcell, E. M., 1949, *J. Chem. Phys.*, **17**, 972.

McCall, D. W. and Hamming, R. W., 1959, *Acta Cryst.*, **12**, 81.

Pake, G. E., 1948, *J. Chem. Phys.*, **16**, 327.

Pake, G. E. and Purcell, E. M., 1948, *Phys. Rev.*, **74**, 1184.

Van Vleck, J. H., 1948, *Phys. Rev.*, **74**, 1168.

27

DECAY OF IONIZATION BELOW THE F-LAYER AT NIGHT

P. BANDYOPADHYAY AND S. K. CHATTERJEE

INSTITUTE OF RADIOPHYSICS AND ELECTRONICS, CALCUTTA UNIVERSITY

(*Received, January* 31, 1961)

ABSTRACT. Titheridge's (1959 *b*) experimental results of variation of the total amount of ionization below the night-time *F*-layer have been re-examined. It has been shown that it is not possible, on the basis of the above results, to discriminate between Titheridge's constant α-model and Mitra's (1957*a*, *b*) time dependent α-model. On other physical grounds, however, it is concluded that while Titheridge's model will possibly hold in the upper part of the region studied, Mitra's model will be valid near the bottom.

1. INTRODUCTION

Ionization in the different ionospheric layers below the *F*-region decays rapidly after sunset and as the plasma frequency f_N of the ionization goes below f_{lim}, the low-frequency limit of the ionosonde—usually 1.0 mc/s—the ionization can no longer be 'seen' in the ionogram. A residual ionization, however, then persists at these levels throughout the night. Recently, Titheridge (1959a) has developed a method of estimating the total amount of this low-lying ionization extending downwards from the bottom of the *F*-layer (where f_N equals 1.0 mc/s) upto *D*-region heights. He has studied by this method its nocturnal variation over Slough and Watheroo in different seasons and at different epochs of the sunspot cycle. The observed variation of the ionization has been interpreted by Titheridge (1959b) to mean that throughout the above height range (200-100 km. roughly) the recombination coefficient remains constant with time around an average value of 1.9×10^{-8} cm^3/sec.

This conclusion of Titheridge, as applied to the lowermost levels of the above height range, is in contradiction with the recombination coefficient model as suggested by Mitra (1957a, b). In the model of Mitra the night-time recombination coefficient, α, at these heights does not remain constant but decreases with time from about 3×10^{-8} cm^3/sec. at sunset to 3×10^{-9} cm^3/sec. at midnight.

It is the purpose of this note to re-examine Titheridge's results on the basis of a possible time variation of the night-time recombination coefficient as in Mitra's model and assumed valid for the whole of the height range in question. It will be shown that the variation of the total amount of the low-lying ionization is insensitive to the α-model used. Consequently, it is not possible, on the basis of Titheridge's results, to discriminate between his 'constant' α-model and

Mitra's 'time dependent' α-model or to find an upper height limit to the range of validity of the latter model. On other physical grounds, however, it can be shown that while Titheridge's model will probably hold for the upper part of the height range in question, Mitra's model will be valid near the bottom.

2. INTERPRETATION OF RESULTS

For α constant in time, the nocturnal variation of the total amount of the low-lying ionization is given by

$$\frac{n(t)}{n(0)} = \frac{1}{1+\alpha N_0 t} \qquad \ldots \quad (1)$$

where $n(t)$ is the value of the total ionization at any time t and $n(0)$ the value of the same at sunset ($t = 0$) and αN_0 is assumed constant with height.

Curves marked T_1, T_2, and T_3 in Fig. 1 show this variation for three possible values of αN_0 chosen by Titheridge, namely 0.5×10^{-3} sec. ^{1}, $1.0\times10^{-3}\text{sec}^{-1}$ and $2.0\times10^{-3}\,\text{sec}^{-1}$. His conclusion about constancy of α with time from sunset to midnight is based on the fact that the different sets of his experimental points

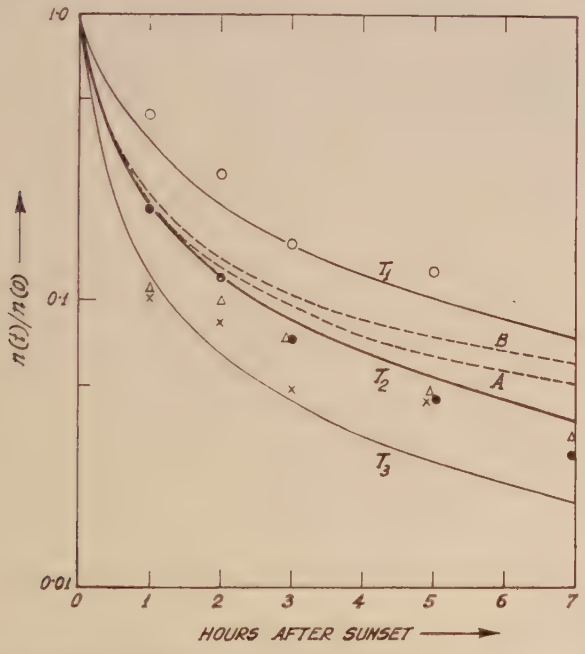

Fig. 1. Relative amount of ionization below night-time F-layer. Solid lines show the variation after Titheridge for three different values of αN_0 when α is independent of time. Broken lines show the variation for the same initial value of αN_0 as the curve marked $T2$ but with α dependent on time. Open circles, filled circles, triangles, and crosses indicate different sets of experimental values obtained by Titheridge.

(circles, triangles and crosses in Fig. 1) for these hours follow theoretical curves of the above type fairly closely.

When, however, α is time dependent, we may proceed to calculate the variation of the total amount of the low-lying ionization as follows :

We may put, following Mitra (1954)

$$\alpha = \alpha_0 \epsilon^{-pt}$$

or since p is small

$$\alpha = \alpha_0 - mt \qquad \ldots \quad (2)$$

where α_0 is the value of α at sunset.
Integration of the continuity equation,

$$\frac{\partial N}{\partial t} = -\alpha N^2 \qquad \ldots \quad (3)$$

with α as given by (2) yields

$$N = \frac{N_0}{1 + \left(\alpha_0 - \frac{mt}{2}\right) N_0 t} \qquad \ldots \quad (4)$$

where N_0 is the value of N at sunset. The total amount of the low-lying ionization at any time t is then given by

$$n(t) = \int_0^{h_1} N dh = \int_0^{h_1} \frac{N_0 dh}{1 + \alpha_0 N_0 t - \frac{1}{2} m N_0 t^2} \qquad \ldots \quad (5)$$

where, as mentioned already, h_1 is the height at which $f_N = 1.0$ mc/s.

Integration of (5) requires an advance knowledge of the sunset electron density distribution N_0. First we use a simplified model (broken line curve of Fig. 2) in which in the height range of our interest (200 km–100 km roughly) N_0 is constant. This may be taken as the idealization of an actual profile (full line) given in Fig. 2. Assuming after Titheridge that $\alpha_0 N_0$ has no height variation

$$\frac{n(t)}{n(0)} = \frac{1}{1 + \alpha_0 N_0 t - \frac{1}{2} m N_0 t^2} \qquad \ldots \quad (6)$$

The decay of the total ionization represented by Eq. (6) is shown in Fig. 1 (curve marked A).

The value of m used is 4.9×10^{-15} cm^3/sec^2. It is taken from Mitra's (1957a) experimental model based on the critical frequency data of the night-time E-layer at Watheroo. $\alpha_0 N_0$ is chosen as 1.0×10^{-3}/sec. to correspond to one of Titheridge's curves (marked T2) in Fig. 1. Since Titheridge's average value of α_0 is 1.9×10^{-8} cm^3/sec. the above choice of $\alpha_0 N_0$ yields N_0 as 5.3×10^4/cm^3.

A comparison of the curve marked T2 with that marked A in Fig. 1 shows that for the first few hours after sunset the difference between the two modes of decay—one with 'constant α' and the other with 'time dependent α'—does not become appreciable.

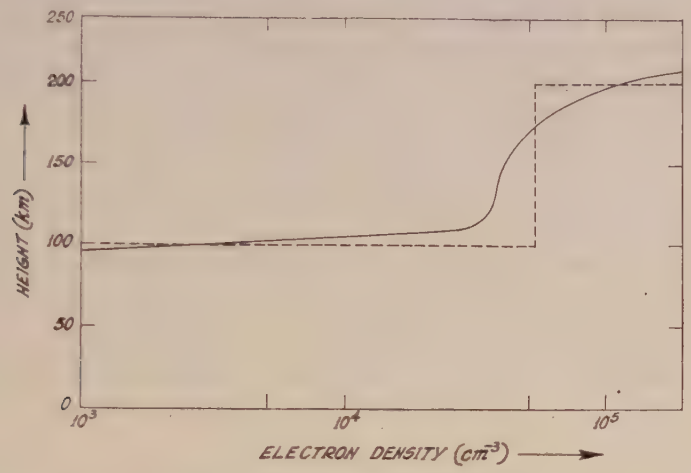

Fig. 2. Electron density distribution at sunset. Broken line curve is the idealization of an actual distribution shown by full line.

Instead of using the idealized profile of Fig. 2 we may take the actual distribution of ionization shown in the same figure. This distribution has been given by Titheridge for Watheroo at 5 minutes before sunset. Taking this to be the sunset distribution we have calculated, using Eq. (4), the ionization profiles at Watheroo for successive hours after sunset. The variation of $\frac{n(t)}{n(0)}$, as obtained by numerical integration of these profiles for heights below 200 km, is shown in Fig. 1 (curve marked *B*). The close agreement between this curve and those marked *T2* and *A* is again noticeable.

Fig. 1 shows that the difference between the modes of decay represented by the curves marked *T2*, *A* and *B*, becomes appreciable only when observations are continued for sufficiently long hours. One may expect, therefore, that data for the later hours may be useful in distinguishing between them. At such hours, however, the situation becomes complicated by the preponderance of another factor, so far neglected, namely, the effect of vertical drift of ionization.

In the preceding calculations we have used Mitra's time-dependent α-model for the whole of the height range from the bottom of the *F*-layer down to *E*-region heights. But that is just to show the insensitiveness of Titheridge's results to the recombination coefficient model chosen. On physical grounds, however, the time dependent α-model of Mitra cannot be used much beyond *E*-region heights. Its essential feature, namely, the time-dependence of α, is due to the

slow emergence of metallic ions of the type X^+ which have a very low value of the recombination coefficient ($\sim 10^{-12}$ cm^3/sec). These ions are, most probably, meteoric in origin. Although their distribution with height is not precisely known, it is believed that their concentration will not be appreciable much above 120 or 130 km. In the absence of these ions X^+ in the higher regions, which extend up to the bottom of the F-layer, electron annihilation at night will take place, as in day-time, through dissociative recombination of the positive molecular ion 0_2^+. For this case, therefore, we may use Mitra's (1959) day-time model, namely.

$$\alpha = \frac{2\times 10^{-19} n(0_2)}{2\times 10^{-11} n(0_2) + 1\times 10^{-8} N}$$

where $n(0_2)$ is the concentration of neutral oxygen molecules and N is the electron density.

At first sight, it may appear that here too, α will be time-dependent because it includes electron-density N, which is variable. Actually, however, this is not so. The electron density of the low-lying ionization is always small. Hence the term involving N in the denominator of the above expression for α will remain negligible compared to the neutral particle density term upto considerable heights. Even at 200 km, near the bottom of the F-layer, and with N as 5×10^4/cm^3, a typical value, the particle density term is more than five times greater than the electron density term. Consequently, α in this region will be sensibly constant with time.

Finally, therefore, it seems probable that while the recombination coefficient has a substantial night-time variation at E-region heights up to the level where meteoric contribution to ionization has an appreciable value, in the region above and extending up to the bottom of the F-layer the coefficient is practically independent of time.

ACKNOWLEDGMENTS

The work forms part of the programme of the Radio Research Committee of the Council of Scientific and Industrial Research. We are indebted to Professor J. N. Bhar for advice and to Dr. A. P. Mitra for helpful discussions.

REFERENCES

Mitra, A. P., 1954, Scientific Report No. 68, Ionosphere Research Laboratory, Pennsylvania State University.

Mitra, A. P., 1957*a*, *J. Atmosph. Terr. Phys.*, **10**, 140.

Mitra, A. P., 1957*b*, *J. Atmosph. Terr. Phys.*, **10**, 153.

Mitra, A. P., 1959, *J. Geophys. Res.*, **64**, 733.

Titheridge, J. E., 1959*a*, *J. Atmosph. Terr. Phys.*, **17**, 110.

Titheridge, J. E., 1959*b*, *J. Atmosph. Terr. Phys.*, **17**, 126.

28

TRANSMISSION CHARACTERISTICS OF PULSE-SLOPE-MODULATED SIGNALS THROUGH BAND-LIMITED SYSTEMS

J. DAS

INDIAN INSTITUTE OF TECHNOLOGY, KHARGPUR

(*Received, October* 31, 1960)

ABSTRACT. Distortion, crosstalk and noise characteristics of P.S.M. have been determined. Maximum harmonic distortion is about 2 per cent for slow cut-off rate of the medium and about 5% for sharp-cut-off filters. Slicers introduce more distortion and non-linearity in modulation. Crosstalk ratios are better than those in P.A.M. for slow cutt-off rate and improvement in crosstalk may be affected by simultaneous introduction of h.f. and l.f. cut-offs. Output S/N ratios show considerable threshold effect and are approximately proportional to the square root of the video bandwidth.

I. INTRODUCTION

The important parameters of a pulse are its amplitude, duration, phase, frequency and slope of the leading and trailing edges. In P.A.M., P.L.M., P.P.M. and P.F.M. systems, the slope is preferably maintained constant at a very high value, whereas in Pulse-slope-modulation (Das, 1954), the slope is varied in accordance with the modulating signal, keeping other parameters constant. The modulating signal is recovered by differentiation and 'Box-car' demodulation

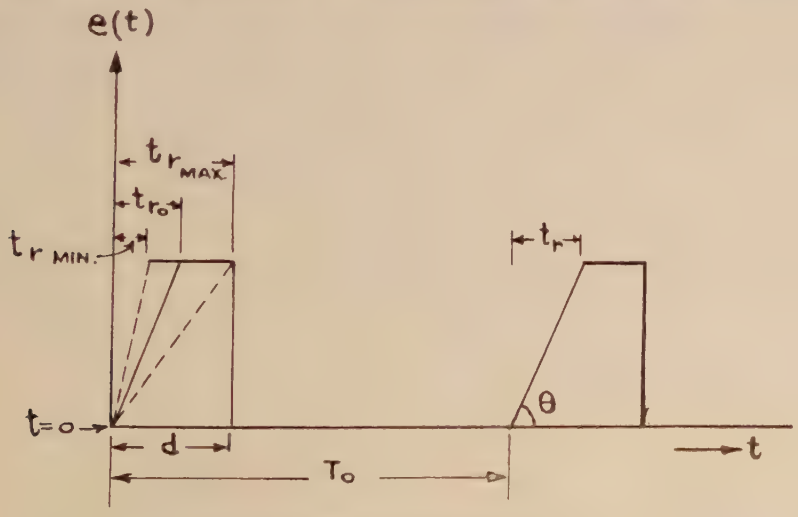

Fig. 1(a). P. S. M. signal. Ch. 1.

of the slope-modulated pulses. The frequency spectrum (Das, 1955) of the P.S.M. signal is given by Fig. 1(a) & 1(b):

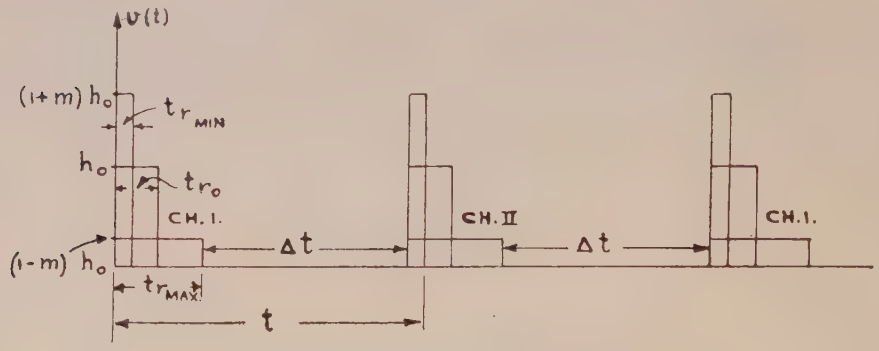

Fig. 1(b) Differentiated signal. Ch. I and Ch. II.

$$F(t) = \frac{Ad}{T_0} - \frac{At_{r_0}}{2T_0(1+m\sin\phi)} + \frac{2A}{T_0}\sum_{n=1}^{\infty}\frac{\sin\omega n(d-t)}{\omega n}$$

$$+\frac{2A}{T_0}\sum_{n=1}^{\infty}\frac{(1+m\sin\phi)}{t_{r_0}\omega^2 n^2}\left[\cos\omega n\left\{t-\frac{t_{r_0}}{(1+m\sin\phi)}\right\}-\cos\omega nt\right] \quad \ldots \quad (1)$$

where,

t_{r_0} = mean risetime

m = modulation index $= \dfrac{t_{r_{max}} - t_{r_{min}}}{t_{r_{max}} + t_{r_{min}}}$

$\omega = \dfrac{2\pi}{T_0}$

$E\sin\phi$ = modulating voltage.

The differentiated signal consists of a pulse train containing both amplitude modulation and inverse width modulation, as is seen from

$$F'(t) = \frac{2A}{T_0}\sum_{n=1}^{\infty} -\cos\omega n(t-d)$$

$$+\frac{2A}{T_0}\sum_{n=1}^{\infty}\frac{(1+m\sin\phi)}{t_{r_0}\omega n}\left[\sin\omega n\left\{\frac{t_{r_0}}{(1+m\sin\phi)}-t\right\}+\sin\omega nt\right] \ldots \quad (2)$$

The inverse width modulation is however cancelled by the use of the 'Box-car' demodulator and the audio output is due only to the amplitude modulation of the differentiated pulses.

Usefulness of a transmission system is determined by the effects of non-ideal circuits and limited bandwidth on its various characteristics—specially audio distortion, crosstalk and noise. These have been discussed here for a P.S.M. system. Since the slope distortion due to limited bandwidth occurs before the 'Box-car' circuit, the effect of both amplitude modulation and inverse width modulation has to be considered for the purpose of determining harmonic distortion and crosstalk. We can generally assume that the system is linear and passive up to the differentiator and on this basis, calculate the theoretical harmonic distortion and crosstalk in the system. For determining the effect of noise, the slope variation only due to noise pulses is calculated for different bandwidths.

The experimental set-up used for the determination of various characteristics had the following specifications (Fig. 2) :

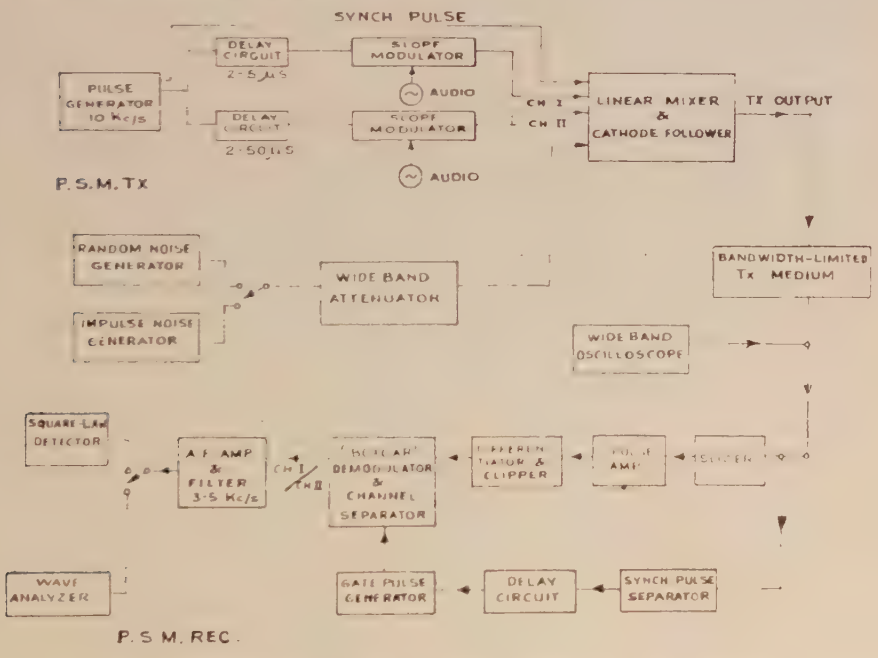

Fig. 2. Experimental set-up—P.S.M. Transmitter and Receiver.

P.R.F. = 10Kc/s. $= 1/T_0$
Pulse duration $d = 2-15\ \mu$ sec.
Mean risetime $t_{r_0} = 1-5\mu$ sec.
Delay between Ch. I and Ch. II $= 2-50\ \mu$ sec.
System bandwidth = 1 Mc/s.

Audio frequency passband = 0 to 3.5 Kc/s

A.F. modulating frequency = 1 Kc/s.

The modulation was linear for an audio volume range of 40 db. The total harmonic distortion in the received audio output was 2.0% with the peak detector and 0.8% with the 'Box-car' demodulator for a modulation range of 35 db. The inherent crosstalk and noise in the system was approximately 65 db below the signal level.

II. DISTORTION

Harmonic distortion occurs due to non-ideal differentiators, high frequency cut-off, low frequency cut-off and due to the use of slicers for elimination of noise. An ideal differentiator gives an output amplitude equal to τ_1/t_r, where τ_1 is a constant. But with a simple R—C differentiator, the amplitude of the differentiated pulses is given by

$$V(t) = \frac{\tau_1}{t_r}\,[\,1 - \exp\,(-t/\tau_1)] - \frac{\tau_1}{t_r}\left[1 - \exp\left\{-\frac{(t-t_r)}{\tau_1}\right\}\right] . U(t-t_r) \quad \ldots \quad (3)$$

where $U(t-t_r)$ = Unit step function starting at $t = t_r$, and $\tau_1 = RC$ of the differentiator.

It is thus seen that the output signal does not reach its peak value immediately and with large τ_1, the peak value will not be reached at all for small values of t_r. Due to the associated inverse width modulation, the sharper pulses, corresponding to the peaks of the modulating voltage, will be more attenuated than the wider pulses and the resulting audio output will have its peaks flattened. The use of a peak detector then will give rise to pronounced second harmonic distortion. However, with a 'Box-car' pulse-lengthener circuit, the narrow gate pulse is arranged to occur at $t \leqslant t_{r_{min}}$ and the amplitude of the output pulses becomes proportional to $(1/t_r)$. With gate pulses narrower than the differentiated pulses, the harmonic distortion is very small even for large values of τ_1, as shown in Fig. 3. The experimental total distortion for the peak detector, also shown in Fig. 3, agrees sufficiently with the theoretical values calculated from Eq. (3).

A transmission medium with 6db/octave high frequency cut-off rate, simulated by a simple RC-lowpass filter, gives a differentiated output:

$$V(t) = \frac{\tau_1}{t_r}\left[1 - \exp\left(-\frac{t}{\tau_2}\right)\right] \quad \frac{\tau_1}{t_r}\left[1 - \exp\left\{-\frac{(t-t_r)}{\tau_2}\right\}\right] . U(t-t_r) \qquad (4)$$

where

τ_1 = differentiation constant; $\tau_2 = RC$ of the lowpass filter.

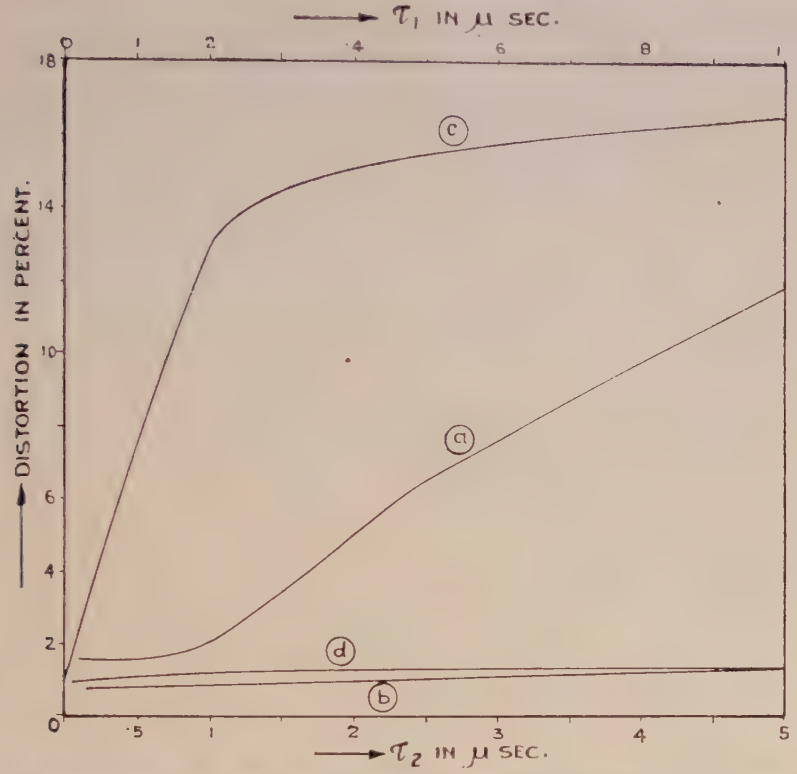

Fig. 3. Experimental total distortion with R–C differentiators and lowpass filters.
$d = 10\mu$sec, $tr_0 = 1.8\mu$ sec, $m = 0.82$, Input level $= -3db$.
(a) For R–C differentiator having different τ_1 using Peak detector.
(b) „ „ „ „ „ „ 'Box-car' circuit.
(c) For R–C l.p. filter having different τ_2 using Peak detector.
(d) „ „ „ „ „ „ 'Box-car' circuit.

As in the case of Eq. (3), the peak amplitude reached by the pulses of different widths will not be proportional to τ_1/t_r and with a peak detector, there will be considerable second harmonic distortion. But with a 'Box-car' circuit, arranged to gate at $t \leqslant t_{rmin}$, the distortion is very much minimised, as is seen in Fig. 3.

With transmission media, having sharp high frequency cut-off, the pulse response is oscillatory and considerable distortion occurs with a peak detector. With the 'Box-car' demodulator circuit, the gate pulse is arranged to occur before the oscillation starts; even then, the amplitude of the output pulses is not strictly proportional to τ_1/t_r and there is some distortion in the audio output. The experimental results, as shown in Fig. 4, have been obtained with a variable cut-off electronic filter having 18 db/oct. and 36 db/oct. slopes.

The effect of low frequency cut-off, having sharp as well as slow rate of cut-off, is rather small. Theoretically, the peak amplitude of the differentiated pulses

occurs at $t = 0$, and the audio output is distortionless. But with higher cut-off frequency, there is a trailing-edge overshoot (Bhattacharyya, 1953) with distorted

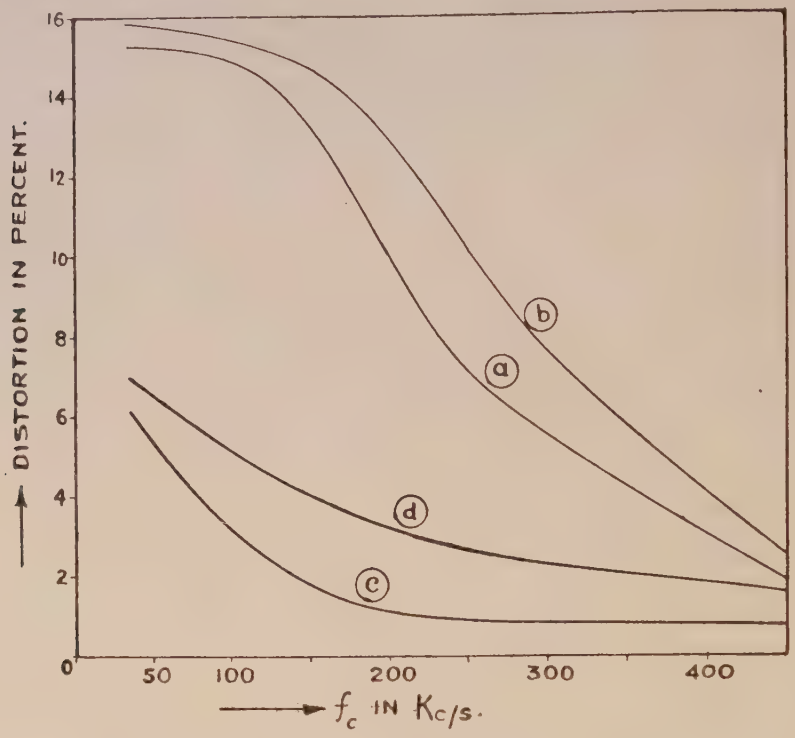

Fig. 4. Experimental total distortion with lowpass electronic filter.
$d = 10\mu$ sec, $tr_0 = 1.8\mu$sec, $m = 0.82$; Input level $= -3db$.
(a) With $18db$/oct cut-off using peak detector.
(b) With $36db$/oct ,, ,, ,, ,,
(c) With $18db$/oct ,, ,, 'Box-car' circuit.
(d) With $36db$/oct ,, ,, ,, ,,

modulation on it. With a peak-detector, this gives rise to certain distortion in the audio output, whereas, the 'Box-car' circuit nullifies the effect of the trailing-edge modulation and the output has very little distortion—approximately 1% only for all practical bandwidths.

A slicing circuit introduces some more non-linearity in modulation and harmonic distortion in the audio output. From noise considerations, the slicing level is generally maintained at half the height of the received pulses. Due to slicing, the differentiated pulses are time-displaced and even after 'Box-car' demodulation, some amount of distorted pulse-length-modulation occurs. However, on further analysis, it is found that the overall distortion due to this P.L.M. is always less than 2%.

The distortion caused by the lowpass band-limited system in the sliced output is rather serious. For pulses with small t_r, the half level is reached much after t_r and the corresponding slope is less than that attained by the unsliced distorted pulses. This makes it necessary to lower the slicing level such that the slicing time $t_s \leqslant t_{r_{min}}$. Fig. 5 shows the nature of the distortion obtained at optimum slicing levels corresponding to the different values of τ_2 and f_c. For highpass filters, the slicer circuits do not contribute to any further distortion, as has been verified experimentally.

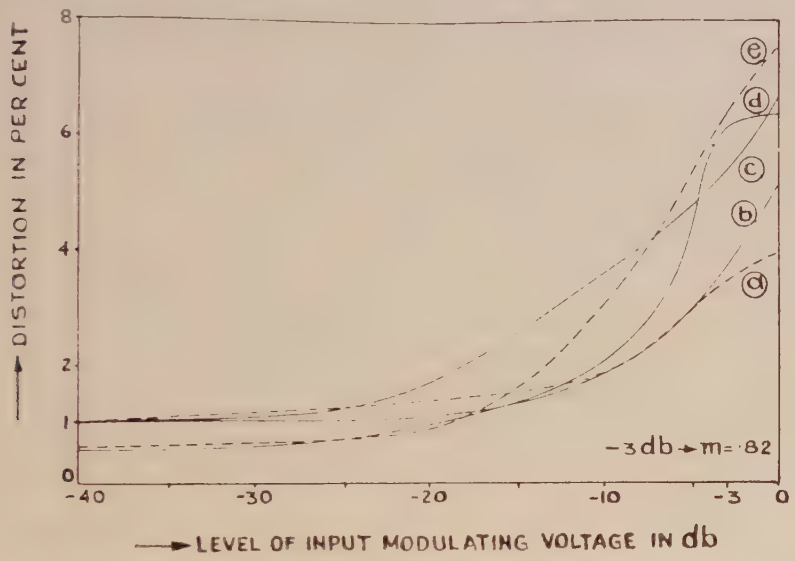

Fig. 5. Experimental total distortion with sliced inputs using 'Box-car' circuit for lowpass filters having different τ_2 and f_c.

$d = 10\mu S$, $tr_0 = 1.8\mu S$, Input level $= -3db$ for $m = 0.82$.

(a) With R–C l.p. filter (6*db*/oct); $\tau_2 = 0.5\mu$sec; $h_s = 0.5h_0$.

(b) With „ „ „ „ $\tau_2 = 1\mu$sec; $h_s = 0.36h_0$.

(c) With „ „ „ „ $\tau_2 = 3\mu$sec; $h_s = 0.15h_0$.

(d) With electronic l.p. filter, $f_c = 200$ Kc/s; 18*db*/oct slope; $h_s = 0.6h_0$.

(e) With electronic l.p. filter; $f_c = 200$ Kc/s; 36*db*/oct slope; $h_s = 0.6h_0$

III. CROSSTALK

Due to limited bandwidth, amplitude and phase distortion occur to the transmitted pulses and there is normally a carry-over of energy from one pulse to the following pulses. The crosstalk thus developed, may be caused either by high frequency cut-off or by low frequency cut-off. For high frequency cut-off

with 6 db/oct. slope, simulated by an R–C lowpass filter, the peak-to-peak carry-over voltage is found to be

$$C_0(t) = h_0 \exp\left(-\frac{t}{\tau_2}\right)\left[(1+m)\left\{\exp\left(\frac{t_{r_{min}}}{\tau_2}\right)-1\right\} -(1-m)\left\{\exp\frac{t_{r_{max}}}{\tau_2}\right)-1\right\}\right] \quad \ldots (5)$$

where h_0 = mean height of the differentiated pulses,
$\tau_2 = RC$ of the lowpass filter.

The crosstalk ratio is then given by

$$\text{C.T. ratio} = \frac{2m \cdot \exp(t/\tau_2) \cdot \left[1-\exp\left(-\frac{t_{r_{min}}}{\tau_2}\right)\right]}{\left[(1+m)\left\{\exp\left(\frac{t_{r_{min}}}{\tau_2}\right)-1\right\}-(1-m)\left\{\exp\left(\frac{t_{r_{max}}}{\tau_2}\right)-1\right\}\right]} \quad \ldots (6)$$

Since for high frequency cut-off, $C_0(t)$ decreases rapidly with time, it is only necessary to consider the carry-over voltage from the channel pulse previous to the signal pulse. The numerical evaluation of Eq.(5) shows that $C_0(t)$ is of opposite phase to that of the signal voltage. The experimental values of crosstalk ratios, with $d = 10\ \mu$ sec, $t_{r_0} = 1.82\ \mu$ sec and $m = 0.82$, are shown in Fig. 6 for various values of τ_2 and the channel separation Δt. These results agree closely with values obtained from Eq.(6).

For low frequency cut-off with 6 db/oct. slope, the crosstalk ratio for the carry-over voltage from the single previous channel (τ_3 small) is given by :

$$\text{C.T.ratio} = \frac{2m \cdot \exp\left(\frac{t-t_{r_{min}}}{\tau_3}\right)}{\left[(1+m)\left\{1-\exp\left(\frac{t_{r_{min}}}{\tau_3}\right)\right\}-(1-m)\left\{1-\exp\left(\frac{t_{r_{max}}}{\tau_3}\right)\right\}\right]} \quad \ldots (7)$$

where $\tau_3 = RC$ of the highpass filter.

The carry-over vltage in this case is found to be of the same phase as that of the signal voltage. The experimental results with small values of τ_3 are also shown in Fig. 6 and they agree sufficiently with the results of Eq. (7).

As the coupling and decoupling circuits of pulse amplifiers are generally made large, the carry-over voltages from other previous channels have also to be considered to determine the net crosstalk ratio. With certain simplifying assumptions, it is found that the crosstalk ratio now is given by

$$\text{C.T. ratio} = \frac{2m\omega_m\tau_3 T_0}{[(1-m)t_{r_{max}}-(1+m)t_{r_{min}}]} \quad \ldots (8)$$

where ω_m = modulating angular frequency $\ll 1/T_0$; and $T_0 \ll \tau_3$. This result is similar to that obtained in case of P.A.M. (Flood, 1951). The carry-over voltage now is of opposite phase to that of the signal voltage.

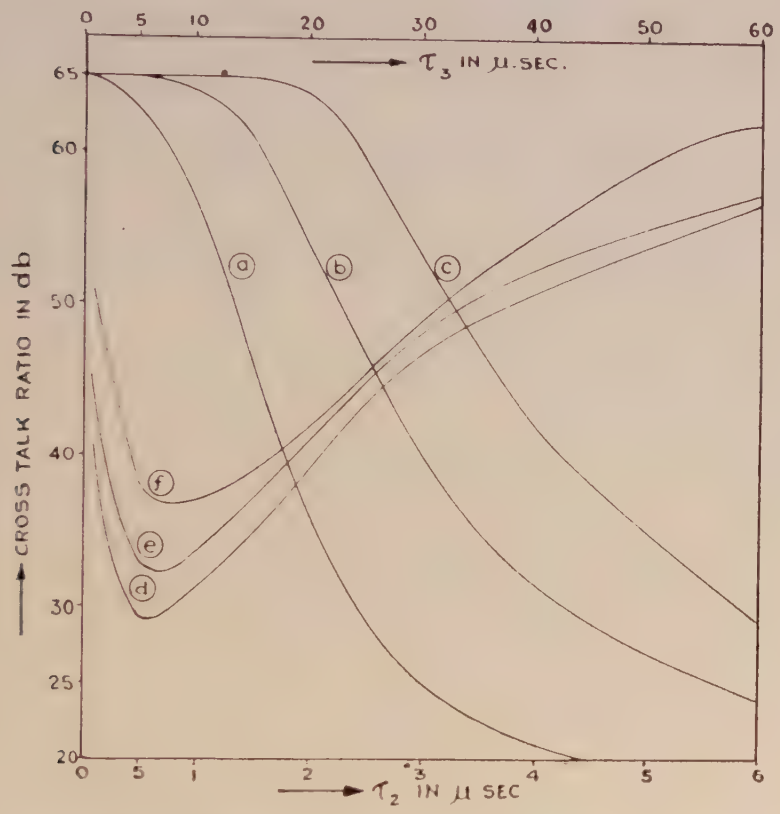

Fig. 6. Experimental crosstalk ratios with R–C filters for various τ_2, τ_3 and channel separation Δt.

$d = 10\ \mu S$, $tr_0 = 1.8\ \mu S$, $m = 0.82$, Input level $= -3db$.

(a) For R–C l.p. filter (τ_2) (6db/oct), $\Delta t = 5\ \mu$ sec.

(b) ,, ,, ,, ,, , $\Delta t = 10\ \mu$ sec.

(c) ,, ,, ,, ,, , $\Delta t = 15\ \mu$ sec.

(d) For R–C h.p. filter (τ_3) (6db/oct), $\Delta t = 5\ \mu$ sec.

(e) ,, ,, ,, ,, , $\Delta t = 10\ \mu$ sec.

(f) ,, ,, ,, ,, , $\Delta t = 15\ \mu$ sec.

Since with reference to the phase of the signal voltage, the carry-over voltage due to h.f. cut-off is of opposite phase and that due to l.f. cut-off with small

values of τ_3 is of same phase, it is possible to minimise crosstalk by using simultaneous h.f. and l.f. cut-offs. The crosstalk ratio is now found to be

C.T. ratio

$$= \frac{2m\left[\exp\left(-\frac{t_{r_{min}}}{\tau_3}\right) - \exp\left(-\frac{t_{r_{min}}}{\tau_2}\right)\right]}{\left\{(1+m)\left[\exp\left(-\frac{t}{\tau_3}\right)\left\{1-\exp\left(\frac{t_{r_{min}}}{\tau_3}\right)\right\} - \exp\left(-\frac{t}{\tau_2}\right)\left\{1-\exp\left(\frac{t_{r_{min}}}{\tau_2}\right)\right\}\right]\right.}$$

$$\left. -(1-m)\left[\exp\left(-\frac{t}{\tau_3}\right)\left\{1-\exp\left(\frac{t_{r_{max}}}{\tau_3}\right)\right\} - \exp\left(-\frac{t}{\tau_2}\right)\left\{1-\exp\left(\frac{t_{r_{max}}}{\tau_2}\right)\right\}\right]\right\} \quad \ldots (9)$$

The C.T. ratio will be maximum for certain relative values of τ_2 and τ_3. It is also possible to forecast the relative values of matching τ_2 and τ_3 for a certain channel separation Δt, as is given by

$$\Delta t = \left[\frac{\tau_2\tau_3}{\tau_3-\tau_2} \cdot \ln\left(\frac{D-C}{A-B}\right)\right] - [t_{r_{max}} + t_{r_{min}}] \quad \ldots (10)$$

where, $A = \frac{(1+m)}{\tau_3}\left[\exp\left(\frac{t_{r_{min}}}{\tau_3}\right) - 1\right]$

$$B = \frac{(1-m)}{\tau_3}\left[\exp\left(\frac{t_{r_{max}}}{\tau_3}\right) - 1\right]$$

$$C = \frac{(1+m)}{\tau_2}\left[1-\exp\left(\frac{t_{r_{min}}}{\tau_2}\right)\right]$$

$$D = \frac{(1-m)}{\tau_2}\left[1-\exp\left(\frac{t_{r_{max}}}{\tau_2}\right)\right]$$

Experimental results with simultaneous h.f. and l.f. cut-offs are shown in Fig. 7 and they agree closely with the results of Eq.(9) and of Eq. (10).

The pulse response with sharp cut-off filters is oscillatory (Guillemin, 1935) and the peak-to-peak carry-over voltage, for uniform transmission upto ω_c, is given by

$$C_0(t) = \frac{h_0}{\pi}\{2m \cdot Si(\omega_c t') - (1+m) \cdot Si[\omega_c(t'-t_{r_{min}})]$$

$$+(1-m) \cdot Si[\omega_c(t'-t_{r_{max}})]\} \quad \ldots (11)$$

where, $t' = t - t_d = (\Delta t + t_{r_{max}} + t_{r_{min}})$;

$-t_d\omega$ = phase shift within the pass band;

$t_d \cong \pi/\omega_c$

The crosstalk ratio is now $[4mh_0 f_c \cdot t_{r_{min}} \cdot \ell'_0(t)]$. The oscillatory nature of the C.T. ratio is shown in the experimental results of Fig. 8, obtained with an electronic filter.

In case of highpass sharp cut-off filters, the crosstalk ratio is given by

$$\text{C.T. ratio} = \frac{2m\pi}{\{(1+m) \cdot Si[\omega_c(t'-t_{r_{min}})] - (1-m) \cdot Si[\omega_c(t'-t_{r_{max}})] - 2m \cdot Si(\omega_c t')\}} \quad \ldots \quad (12)$$

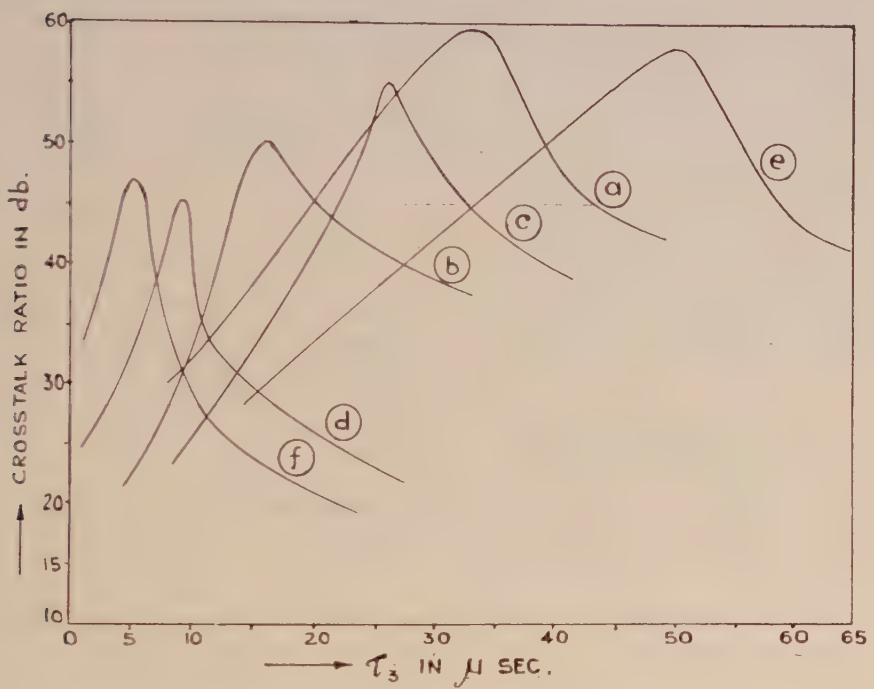

Fig. 7. Experimental crosstalk ratios due to combined H.F. and L.F. cut-off.
τ_2 = R–C of l.p. filter; τ_3 = R–C of h.p. filter; $d = 10\ \mu S$, $m = 0.82$.

(a) $\Delta t = 5\ \mu S$; $\tau_2 = 1\mu S$ (d) $\Delta t = 10\ \mu S$; $\tau_2 = 6\ \mu S$

(b) $\Delta t = 5\ \mu S$; $\tau_2 = 2\mu S$ (e) $\Delta t = 15\ \mu S$; $\tau_2 = 3\ \mu S$

(c) $\Delta t = 10\ \mu S$; $\tau_2 = 3\mu S$ (f) $\Delta t = 15\ \mu S$; $\tau_2 = 8\ \mu S$

Here the oscillations start only after the cut-off frequency becomes comparable with the pulse repetition frequency. Since the carry-over voltage due to both highpass and lowpass filters are oscillatory, it is possible to minimise crosstalk by simultaneous use of h.f. and l.f. cut-offs. In Fig. 8, certain minima on the C.T. ratio-curve could be improved to the points X_1', X_2', ... etc. by the use of highpass filters having suitable cut-off frequencies. The values of the cut-off frequencies fc_2 for the highpass filters are indicated on the same figure.

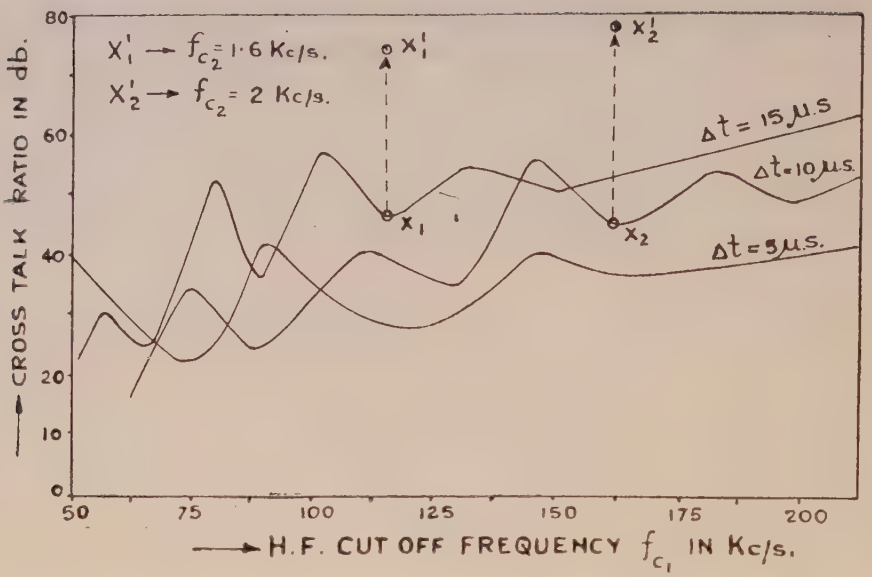

Fig. 8. Experimental crosstalk ratios due to electronic lowpass filter having 18*db*/oct. slope.

$d = 10\mu S$; $m = 0.82$; f_{c_1} = cut-off frequency of l.p. filter.

f_{c_2} = cut-off frequency of h.p. filter.

X'_1 = Improved C.T. ratio with simultaneous use of l.p. and h.p. filters, $f_{c_2} = 1.6$ Kc/s.

X'_2 = Improved C.T. ratio with simultaneous use of l.p. and h.p. filters, $f_{c_2} = 2$ Kc/s.

When the slicer circuit is used, the slopes contain whatever carry-over voltages already present and the only difference is in the time of differentiation. Due to slicing, the differentiated pulses correspond to the slopes at a time later than $t = 0$, but the effective crosstalk ratios are not affected.

IV. NOISE

In case of random noise, the effective noise modulation with sharp cut-off media has been shown to be (Das, 1956)

$$(\Delta \tan \theta_N)_{eff.} = 0.1148\, f_c \times N(\text{peak}) \qquad \ldots \quad (13)$$

where, $\Delta \tan \theta_N = (\tan \theta_N - \tan \theta_{(mean)})$

$N_{(peak)}$ = peak amplitude of noise pulses

f_c = cut-off frequency.

The total audio noise power accepted by the a.f. amplifier is then proportional to

$$\frac{(\Delta \tan \theta_N)^2_{eff}.F_a}{f_c} \propto \left[\frac{t_{r_0}^2}{T_0^2} + \left(\frac{2}{\pi^2}\right) \cdot \sum_{n=1}^{T_0 f_c} \frac{1}{n^2} \cdot \sin^2 \left(\frac{\pi n t_{r_0}}{T_0} \right) \right] \quad \ldots \quad (14)$$

Numerical evaluation of Eq.(14), with $t_{r_0} = 1\ \mu$ sec, $d = 10\ \mu$ sec, $m = 0.9$, $f_c = 1$ Mc/s and F_a = audio passband = 0 to 3.5 Kc/s, shows that

$$\frac{\text{R.M.S. audio signal}}{\text{Effective audio noise}} \text{ (in the output)} = \frac{mA}{(1.414T_0) \times 0.0956 (\Delta \tan \theta_N)_{eff.}} \times \left(\frac{f_c}{F_a}\right)^{\frac{1}{2}} \quad \ldots \quad (15)$$

$$= 10.9 \cdot \frac{A}{N_{(peak)}} \cdot$$

This gives an output signal-to-noise ratio in db equal to $\left[20.74 + 20 \log \frac{A}{N_{(peak)}} \right]$.

For the extreme value of $\frac{A}{N_{(peak)}}$ equal to 2, the output signal-to-noise ratio is 26.74 db. After this threshold point, the improvement in the output S/N ratio in db is constant, but approximately varies as $(f_c/F_a)^{\frac{1}{2}}$. The theoretical and experimental results agree favourably as is shown in Fig. 9. The results of the impulse-noise tests show a further improvement in the output S/N ratios.

With transmission media having slower rate of cut-off, the equivalent bandwidth (Cherry, 1949) is determined and the above method is used for calculating the output S/N ratio. For simple $R-C$ lowpass filters, the equivalent cut-off frequency f_c is $1/4\tau$, and the minimum risetime is 2τ. To obtain a bandwidth of 1Mc/s, the time constant τ has to be 0.25 μ sec only.

V. DISCUSSION

Distortion in the P.S.M system has been very much minimized by using 'Box-car' pulse-lengthener circuit. The average distortion does not exceed 2% for media with 6 db/oct. cut-off rate. But for sharp cut-off media, the distortion is upto 5% with larger modulation index. Distortion due to l.f. cut-off is less for all cases. Linearity of modulation and distortion characteristics are poorer when the slicer circuit is used. For higher level of modulation, the percentage distortion exceeds 5% at optimum slicing levels. But in case of P.L.M., Kretzmer (1947)

has shown that even with large video bandwidths and ideal filters and amplifiers, the audio distortion is of the order of 4%. Levy (1949) has reported a P.P.M. system, where the overall distortion in audio characteristics was of the order of 5%. With bandwidth restriction, the distortion increases in P.L.M. and with $\tau_2 = 2\ \mu$ sec, the total distortion is found to be approximately 8% for similar pulse-width and repetition frequency.

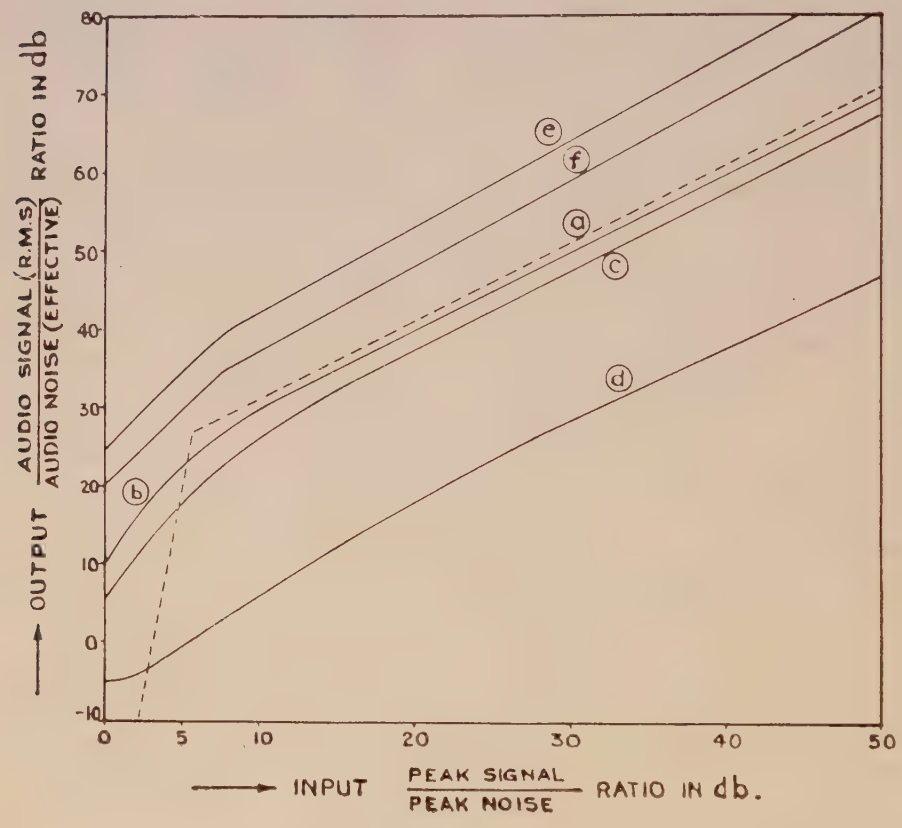

Fig. 9. Improvements in signal-to-noise ratio with sharp cut-off filters using slicers. $d = 10\ \mu$S, $F_a = 3.5$ Kc/s, P.R.F. = 10 Kc/s.

(a) Theoretical S/N ratio with random noise, $f_c = 1$ Mc/s, $t_{r_0} = 1\ \mu$ sec.

(b) Experimental ,, ,, ,, ,, ,, ,, ,,

(c) ,, ,, ,, ,, ,, $f_c = 0.5$ Mc/s; $t_{r_0} = 1.82\ \mu$S.

(d) ,, ,, ,, ,, ,, without slicer, $f_c = 1$ Mc/s.

(e) Experimental S/N ratio with impulse noise, $f_c = 1$ Mc/s; $t_{r_0} = 1\ \mu$S, impulse width = 1μS;, P.R.F. of impulses = 500 c/s.

(f) Experimental S/N ratio with impulse noise, $f_c = 1$ Mc/s; $t_{r_0} = 1\mu$S, impulse width = 1μS; P.R.F., of impulses = 5 Kc/s.

The other advantage of the P.S.M. system is in its better crosstalk characteristics. For a P.A.M. system with same pulse duration, the crosstalk ratio with $R-C$ lowpass filters is given as $\left(8.686 \times \frac{t-d}{\tau_2} \right) db$. In case of P.L.M. and P.P.M. (Deloraine, 1944) there is an approximate improvement factor of $\left(\frac{2t_m}{t_r} \right)$, where t_m is the time displacement due to modulation. From above, the improvement in P.S.M. crosstalk ratios are 10 to 17 *db* over those of P.A.M. and with a similar P.T.M. system, the crosstalk ratios would be at least equal.

In case of $R-C$ highpass filters, Flood (1951) has shown that the crosstalk ratio in P.A.M. is $\left(\frac{\omega_m T_0 \tau_3}{d} \right)$ for large τ_3 and small ω_m. Comparing with Eq. (8), the improvement in the P.S.M. crosstalk ratio with reference to P.A.M. is given by

$$\frac{\text{C.T. ratio in P.S.M.}}{\text{C.T. ratio in P.A.M.}} = \frac{2md}{[(1-m)t_{r_{max}} - (1+m)t_{r_{min}}]} = 44.3 \ db. \qquad \ldots \quad (16)$$

for $d = 2\,\mu$ sec; $t_{r_{max}} = 10\,\mu$ sec; $t_{r_{max}} = 1\,\mu$sec; $m = 0.82$.

Even with the improvements obtained in P.P.M. and P.L.M. (Flood, 1952) the P.S.M. crosstalk ratios would be better.

In Fig. 9. it is seen that above 10 *db* input S/N ratio, the experimental values are only 1.4 *db* below the theoretical values and there is an apparent threshold point at 7 *db* input S/N ratio for 1 Mc/s bandwidth. In a P.L.M. system with same maximum pulse duration and bandwidth, the improvement (Das, 1955) in the output S/N ratio is approximately 33 *db* over the input S/N ratio, whereas in P.S.M., the improvement is only about 21 *db*. However, the P.S.M.noise characteristics are definitely superior to those of P.A.M. and F.M. systems.

As an example of the overall performance of P.S.M., with filter-like transmission media, it is seen from Fig. 8, that the crosstalk ratio could be improved to about 80 *db* with $f_{c_1} = 160$ Kc/s and $f_{c_2} = 2$ Kc/s, and the corresponding distortion from Fig. 4 is only $1.5\% \pm 1\%$ for the highpass filter to be used in tendem. The improvement in the output S/N ratio is now only 16.5 *db*. If, then, the input S/N ratio is about 25 *db*, the total noise plus distortion in the output of the system will be about 3% only. This is a considerable advantage of the P.S.M. system.

Fourier expansion of the trapezoidal pulses shows that the useful modulated harmonic amplitudes vary as $1/n^2$, whereas for rectangular pulses the harmonic amplitudes vary as $1/n$, n being the order of the harmonic of the p.r.f. The P.S.M. signal which consists of trapezoidal pulses will then require a lesser nominal bandwidth for transmission. As the noise characteristics of P.S.M. are slightly

inferior but the crosstalk and distortion characteristics are generally superior to those of P.T.M. systems for smaller bandwidths, P.S.M. will be more useful in low-noise bandwidth-limited systems like partially compensated cables and lines, electronic exchanges and others. If the noise level is low, the slicing level will be low and there will be very little audio distortion in the output.

ACKNOWLEDGMENT

The author records his thanks to Prof. H. Rakshit, D.Sc., F.N.I., for, his kind interest in the work.

REFERENCES

Bhattacharyya, B. K., 1953, *Ind. J. Phys.*, **27**, 269.

Cherry, C., 1949, "Pulses and transients in communication circuits", Chapman and Hall.

Das, J., 1954, *Ind. J. Phys.*, **28**, 449.

Das, J., 1955, *Electronic Engg.*, **27**, 482.

Das, J., 1955, *Electronic Engg.*, **27**, 406.

Das, J., 1956, *Electronic Engg.*, **28**, 16.

Deloraine, E. M. and Labin, E., 1944, *Elec. Communication*, **22**, 91.

Flood, J. E., 1951, *Proc. Inst. of Elec. Engineers*, **98**, Part III, 279.

Flood, J. E., 1952, *Proc. Inst. Elec. Engineers*, **99**, Part. IV, 64.

Guillemin, E. A., 1935, "Communication Networks" Vol. **2**, John Wiley & Sons.

Kretzmer, E. R., 1947, *Proc. I.R.E.*, **35**, 1230.

Levy, M. M., 1949, *J. Brit. Instn. Radio Engineers*, **9**, 386.

29

SPACE GROUPS OF CRYSTALS OF α-,β-AND γ-PICOLINE AT $-180°C$

S. G. BISWAS

Optics Department,

Indian Association for the Cultivation of Science, Calcutta-32

(*Received, March* 28, 1961)

Plate III

ABSTRACT. The dimensions of the unit cell, number of molecules per unit cell and the space groups of crystals of α-, β- and γ-picoline at $-180°C$ have been determined by studying the Debye-Scherrer patterns of the crystals. All the crystals are found to have the monoclinic lattice. The space group assigned to the α-picoline crystal is P2/m with $a = 9.97$, $b = 10.91$, $c = 10.90$Å, $\beta = 111°54'$, that of β-picoline is $P2_1/m$ with $a = 6.95$, $b = 11.87$, $c = 7.05$ Å, $\beta = 94°12'$ and that of the γ-picoline crystal is $P2_1/c$ with $a = 7.21$, $b = 7.69$, $c = 10.20$ Å, $\beta = 110°42'$.

INTRODUCTION

In continuation of the previous work on the analysis of the Debye-Scherrer patterns of crystals of toluene (Biswas and Sirkar, 1957), pyridine (Biswas, 1958), chlorobenzene and bromobenzene (Biswas, 1958), 1, 3, 5-trichlorobenzene (Biswas, 1957) and ortho-, meta- and paraxylene (Biswas, 1960), the present investigation was undertaken to study the Debye-Scherrer patterns of α-, β- and γ-picoline at $-180°C$ and to find out the dimensions of the unit cell, number and molecules per unit cell and the space group to which the crystals belong.

EXPERIMENTAL

The Debye-Scherrer patterns of crystals of α-, β- and γ-picoline at $-180°C$ were photographed with a low temperature camera used previously (Biswas, 1958). The radius of the camera was derived from the Debye-Scherrer pattern of Al powder and it was found to be 4.50 cm. A Seifert X-ray tube running at 32 KV and 26 mA was used to photograph the patterns. An exposure of three and half hours using Cu Kα radiation was sufficient to record the patterns with appropriate density.

RESULTS AND DISCUSSION

In determining the dimensions of the unit cells of the crystals of these isomers Ito's method (Ito, 1950) was applied and all the crystals were found to belong to the monoclinic system. The crystals could not be assigned to any lattice of

symmetry higher than that of the monoclinic system. Lipson's method (Lipson, 1949) was also tried, but significant constant differences in the values of $\sin^2\theta$ were not observed.

α-Picoline : The Debye-Scherrer pattern due to crystals of α-picoline at −180°C is reproduced in **Fig. 1**, Plate III. The values of $Q\,(1/d^2_{hkl})$, where d_{hkl} is the spacing of the direct lattice calculated from the Debye-Scherrer rings are tabulated in column 1, Table I. The dimensions of the unit cell of the reciprocal lattice which are found to explain all the observed Q-values satisfactorily are :

$$a^* = 0.0916 \qquad \alpha^* = 59°42'$$
$$b^* = 0.0988 \qquad \beta^* = 90°$$
$$c^* = 0.1161 \qquad \gamma^* = 90°$$

The values of Q observed from the photograph and those calculated with the dimensions of the unit cell given above, the intensities and the proposed indices for the reciprocal lattice are also given in Table I. The dimensions of the unit cell of the direct lattice corresponding to the reciprocal lattice are :

$$a = 9.97 \text{ Å}$$
$$b = 10.92 \text{ Å} \qquad \beta = 120°18'$$
$$c = 11.70 \text{ Å}$$

The above cell was reduced further (Buerger, 1958) and the dimensions of the reduced cell are :

$$a = 9.97 \text{ Å}$$
$$b = 10.92 \text{ Å} \qquad \beta = 111°54'$$
$$c = 10.90 \text{ Å}$$

The indices referred to this reduced direct lattice are given in the last column of Table I.

On examining the powder pattern, it was noticed that there was some indication of the preferential orientation of the crystallites with a particular axis orientated around the vertical axis of the specimen. The primitive translation along the preferred axis is found to be about 10.94 Å. This value agrees with the length either of the b-edge or of the c-edge of the reduced unit cell. The positions of the diffraction maxima on the different layer lines, however, indicate that the prefered axis is the b-axis. The layer lines in which the different maxima due to reflections from planes of different indices are actually present are given in Table II. The positions of the maxima in the different layer lines thus confirm the correctness of the indices assigned to the corresponding reflecting planes.

To determine the number of molecules per unit cell the density of the substance at −180°C was determined by the method described earlier (Biswas and

TABLE I

Indexing of the powder pattern of α-picoline crystals

Q (observed)	Q (calculated)	$h'k'l'$ (reciprocal lattice)	hkl (reduced direct lattice)
0.0293 (m)	0.0293	$0\bar{2}1$	101
0.0335 (m)	0.0336	200	020
0.0345 (m)	0.0348	011	$20\bar{1}$
0.0378 (w)	0.0377	$12\bar{1}$	111
0.0388 (w)	0.0390	020	200
0.0420 (m)	0.0416	$20\bar{2}$	$10\bar{2}$
0.0435 (s)	0.0434	210	120
	0.0433	111	$21\bar{1}$
0.0475 (m)	0.0476	120	002
	0.0471	201	210
			$12\bar{1}$
0.0542 (s)	0.0540	002	$20\bar{2}$
0.0665 (m)	0.0665	$03\bar{1}$	201
0.0680 (s)	0.0685	211	$22\bar{1}$
0.0755 (s)	0.0759	021	030
	0.0756	300	$30\bar{1}$
0.0808 (w)	0.0802	$22\bar{2}$	022
	0.0806	$13\bar{2}$	112
0.0880 (m)	0.0876	202	031
		030	300
			$22\bar{2}$
0.0956 (m)	0.0962	130	310
	0.0954	112	
0.1046 (w)	0.1048	113	131
0.1162 (w)	0.1162	$31\bar{2}$	132
0.1172 (w)	0.1172	$04\bar{2}$	202
			222
0.1251 (w)	0.1247	122	123
0.1350 (vw)	0.1344	400	040
			401
0.1390 (vw)	0.1391	$04\bar{3}$	103
	0.1394	022	402
0.1628 (w)	0.1633	330	330
	0.1622	$02\bar{4}$	410
0.1732 (m)	0.1634	420	240
	0.1730	222	123
0.1890 (w)	0.1886	240	420
	0.1884	402	004
0.2086 (w)	0.2090	312	$70\bar{2}$
			$50\bar{2}$
0.2302 (w)	0.2301	023	430
0.2551 (m)	0.2559	403	$20\bar{5}$
0.3025 (w)	0.3024	600	060
0.3230 (w)	0.3226	151	$15\bar{1}$

TABLE II

Layer line	Indices for the maxima present
Zero layer line	$10\bar{1}$
	$20\bar{1}$
	200
	$10\bar{2}$
	002
	$20\bar{2}$
	201
First layer line	111
	$21\bar{1}$
	210
	012
Second layer line	020
	120
	$12\bar{1}$
	$22\bar{1}$

Sirkar, 1957) and was found to be 1.134 gm cm^{-3}. With this value of the density and the dimensions the unit cell given above the number of molecules per unit cell was found to be 8.08. Thus the unit cell contains eight molecules.

It can be easily seen from Table I that there is no restriction regarding reflection from different planes. There is, however, no space group with eight equivalent points not showing any restriction of reflection. The space group $C^1{}_{2h}-P2/m$ does not show any restriction but it has only four equivalent positions with an asymmetric molecule at each position. It is evident, therefore, that there are two molecules forming an asymmetric unit at each equivalent position in the crystals of α-picoline and the space group is $C^1{}_{2h}$.

β-Picoline : The Debye-Scherrer pattern due to crystals of β-picoline at $-180°$C is reproduced in Fig. 2, Plate III. The values of Q observed from the photograph are given in column 1, Table III.

In this case the dimensions of the unit cell of the reciprocal lattice which could explain all the Q-values satisfactorily are :

$$a^* = 0.1833 \qquad \alpha^* = 90°$$
$$b^* = 0.2014 \qquad \beta^* = 90°$$
$$c^* = 0.0843 \qquad \gamma^* = 85°48'$$

The dimensions of the unit cell of the direct lattice with b-axis as the unique axis corresponding to those of the reciprocal lattice are :

$$a = 6.95 \text{ Å}$$
$$b = 7.05 \text{ Å} \qquad \beta = 94°12'$$
$$c = 11.87 \text{ Å}$$

Fig. 1.

Fig. 2.

Fig. 3.

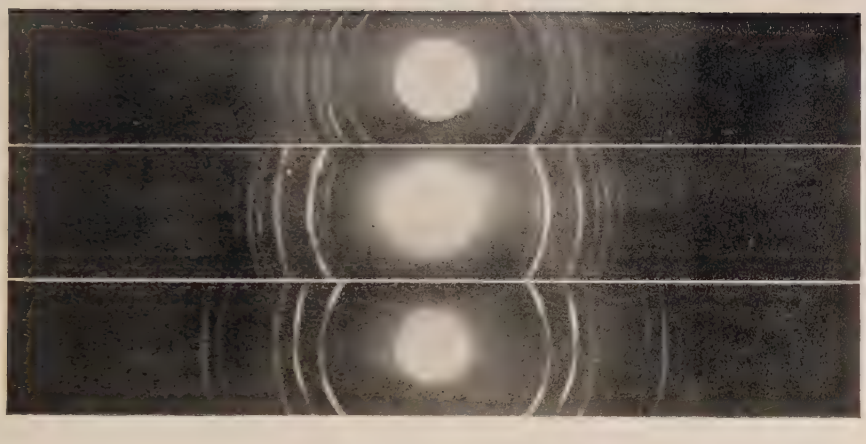

Debye-Scherrer patterns

Fig. 1. α-picoline at − 180°C
Fig. 2. β-picoline at − 180°C
Fig. 3. γ-picoline at − 180°C

It can be easily seen that the above cell cannot be reduced further. So the dimensions of the unit cell of the β-picoline crystal are as given above. The indices of the planes referred to the direct lattice are given in the last column of Table III.

TABLE III

Indexing of powder pattern of β-picoline crystals

Q (observed)	Q (calculated)	$h'k'l'$ (reciprocal lattice)	hkl (final direct lattice)
0.0380 (w)	0.0380	$1\bar{1}0$	$10\bar{1}$
0.0440 (w)	0.0440	110	101
0.0450 (w)	0.0449	$1\bar{1}1$	$11\bar{1}$
0.0495 (s)	0.0493	012	120
0.0510 (vs)	0.0509	111	111
0.0660 (vw)	0.0665	$1\bar{1}2$	$12\bar{1}$
0.0724 (m)	0.0725	112	121
0.0810 (vs)	0.0808	200	002
0.0830 (vs)	0.0832	020	200
0.1020 (s)	0.1018	113	$13\bar{1}$
0.1140 (s)	0.1140	004	040
0.1338 (m)	0.1342	104	041
0.1595 (w)	0.1592	$2\bar{1}3$	132
0.1705 (w)	0.1710	213	132
0.1815 (vw)	0.1818	300	003
0.1875 (vw)	0.1872	030	300
0.2060 (w)	0.2055	$13\bar{1}$	$31\bar{1}$
0.2185 (m)	0.2187	131	311
0.2515 (w)	0.2512	033	330
0.2565 (vw)	0.2560	006	060
0.2900 (m)	0.2900	224	242
0.3015 (w)	0.3012	034	340

The density of the substance at −180°C was found to be 1.098 gm cm^{-3}. The number of molecules per unit cell calculated with this density is found to be 4.01. Thus the unit cell contains 4 molecules. It can be easily seen from Table III that the conditions limiting possible reflections are :

hkl : no condition

hol : no condition

oko : $k = 2n$

So, the probable space group which can be assigned to the crystal is $C^2{}_{2h}$–$P2_1/_m$.

γ-Picoline : The Debye-Scherrer pattern due to crystals of γ-picoline at −180°C is reproduced in Fig. 3, Plate III. The Q-values observed from the photograph are given in column 1, Table IV.

The dimensions of the unit cell of the reciprocal lattice which could account for all the Q-values observed in this case are :

$a^* = 0.1049$ $\quad\quad$ $\alpha^* = 90°$

$b^* = 0.1300$ $\quad\quad$ $\beta^* = 69°18'$

$c^* = 0.1483$ $\quad\quad$ $\gamma^* = 90°$

The dimensions of the unit cell of the direct lattice corresponding to those of the reciprocal lattice after a and c axes being interchanged are :

$a = 7.21$ Å
$b = 7.69$ Å $\qquad \beta = 110°42'$
$c = 10.20$ Å

It can be easily seen that the above cell cannot be reduced further. So, the dimensions of the unit cell of the γ-picoline crystal are as given above. The indices referred to this direct lattice are given in the last column of Table IV.

TABLE IV

Indexing of the powder pattern of γ-picoline crystals

Q (observed)	Q (calculated)	$h'k'l'$ (reciprocal lattice)	hkl (final direct lattice)
0.0450 (vs)	0.0448	200	002
		201	$10\bar{2}$
0.0678 (vs)	0.0676	020	020
0.0880 (s)	0.0880	002	200
0.0888 (m)	0.0888	202	$20\bar{2}$
		201	102
0.1124 (m)	0.1124	220	022
		$22\bar{1}$	$12\bar{2}$
0.1376 (vw)	0.1381	112	211
0.1560 (s)	0.1566	022	220
	0.1564	221	122
		$32\bar{1}$	$12\bar{3}$
		$22\bar{2}$	$22\bar{2}$
0.1768 (w)	0.1768	202	202
		203	$30\bar{2}$
0.1792 (vs)	0.1792	400	004
		$40\bar{2}$	$20\bar{4}$
0.2230 (m)	0.2234	321	123
0.2456 (w)	0.2452	222	222
		401	104
		$40\bar{3}$	304
0.2466 (s)	0.2468	420	024
0.2702 (m)	0.2704	040	040
0.2922 (w)	0.2924	041	140
		$14\bar{1}$	141
0.3142 (s)	0.3146	141	141
0.3588 (vw)	0.3590	$60\bar{2}$	206
	0.3584	042	420
0.3802 (vw)	0.3805	$52\bar{3}$	$32\bar{5}$
0.4500 (m)	0.4496	440	044
0.4705 (vw)	0.4708	620	026
0.4915 (w)	0.4912	604	$40\bar{6}$
0.5432 (w)	0.5437	152	$25\bar{1}$
0.6080 (w)	0.6084	060	060
0.6228 (vw)	0.6222	044	440
	0.6234	602	$20\bar{6}$
0.7120 (m)	0.7120	523	325
0.7245 (m)	0.7241	414	414

The density of the substance at −180°C was found to be 1.163 gm cm^{-3}. The number of molecules per unit cell calculated with this density is found to be 4.03. Thus the unit cell contains four molecules.

Table IV shows that the reflections from the planes (010), (030) and (050) are absent because the Q values for these planes are 0.0169, 0.1521 and 0.4225 respectively and these do not agree with any of the observed values. Hence it is concluded that (*oko*) reflection are absent when k is odd.

The calculated values of Q_{hol} with l odd together with those observed in the neighbourhood of some of these values are given in Table V.

TABLE V

Q_{hol}	Computed	Nearest value observed	Difference
$Q10\bar{1}$	0.0222		
$Q101$	0.0442	0.0450 (002)	+0.0008
$Q20\bar{1}$	0.0772		
$Q10\bar{3}$	0.0898	0.0888 ($20\bar{2}$)	−0.0010
$Q201$	0.1212		
$Q203$	0.1228		
$Q103$	0.1558	0.1560	+0.0002
$Q30\bar{1}$	0.1762	0.1768	+0.0006
$Q301$	0.2422		
$Q203$	0.2548		

The difference between Q_{002} and Q_{101} and that between $Q_{10\bar{3}}$ and $Q_{20\bar{3}}$ are beyond experimental error which is less than 0.0005. Hence (101) and ($10\bar{3}$) reflections are most probably absent. Reflections from the (103) planes may, however, be superposed on that from (220) and the (301) reflection may lie very close to (202) reflection, but since the other (*hol*) reflections with l odd are definitely absent it is concluded that all such reflections are absent.

Table IV then shows the following conditions limiting possible reflections :

hkl : no condition

hol : $l = 2n$

oko : $k = 2n$

So, the probable space group of the crystal is C^5_{2h}—$P2_1/c$.

Finally, it has to be pointed out that in all the cases mentioned above assignment of alternative unit cell dimensions leads to serious difficulties, because either some of the intense reflections cannot be accounted for or the number of molecules per unit cell differs considerably from whole numbers. On the other hand, with cell dimensions given above these difficulties disappear completely.

ACKNOWLEDGMENT

The author is indebted to Professor S. C. Sirkar, D.Sc., F.N.I., for his kind interest and guidance during the progress of this work. The author is also indebted to the Council of Scientific and Industrial Research for financing the scheme under which this work was done.

REFERENCES

Biswas, S. G. and Sirkar, S. C., 1957, *Ind. J. Phys.*, **31**, 141.
Biswas, S. G., 1958, *Ind. J. Phys.*, **32**, 13.
Biswas, S. G., 1958, *Acta Cryst.*, **11**, 882.
Biswas, S. G., 1959, *Ind. J. Phys.*, **33**, 371.
Biswas, S. G., 1960, *Ind. J. Phys.*, **34**, 263.
Buerger, M. J., 1957, *Zeits. f. Krist.*, **109**, 42.
Ito, T., 1950, X-ray studies on polymorphism, (Maruzen Co. Ltd., Tokyo, p. 210-214.)
Lipson, H., 1949, *Acta. Cryst.*, **2**, 49.

BOOK REVIEWS

ORGANIC ELECTRONIC SPECTRAL DATA. Vol. I, 1946-52—By Mortimer J. Kamlet, Editor. Pp. 1208. Interscience Publishers, New York, London, 1960. Price $ 28.50. Vol. II. 1953-55—By Herbert E. Ungnade, Editor, Pp. 919. Interscience Publishers, New York, London, 1960. Price $ 17.50.

These two volumes give the wavelengths of absorption maxima and the values of log(ϵ) in the ultraviolet and visible regions for organic compounds reported by various workers during the years 1946-52 and 1953-55 respectively. It is stated in the preface that the data were taken from 60 chemical and allied journals. The data are given in four columns, the first of which contains the chemical formula and the name of the compound. The solvent or the state in which the spectra have been studied is given in column 2 and the wavelengths of absorption maxima and the values of log(ϵ) at the maxima are given in column 3. The last column gives the reference in which the journal is represented by a number and the paper by another number. The details of the corresponding references are given at the end of each volume. The references are arranged according to the alphabetical order of the names of the journals.

Such data are immensely helpful not only to chemists engaged in research in synthesis or analysis of organic chemicals but also to many physicists who are interested in the electronic spectra of such compounds. To research workers the value of the data depend on the degree of their completeness. The Board of Editors secured contributions from 51 specialists from different countries, and therefore, it has been possible to compile the data from a large number of journals in different languages which are ordinarily not available to many research workers. As stated above, 60 journals in Chemistry and allied subjects have been consulted to compile the data, and evidently, journals in physics have been scrupulously avoided. It is difficult to understand why the Board of Editors assumed that data on electronic spectra of organic compounds cannot be published in journals in physics. In fact, such an assumption only results in omission of certain data which might be useful to research workers. As for instance, it might be pointed out that during the years 1949-1955 a few papers dealing with ultraviolet absorption spectra of some organic compounds were published in this journal and some of these papers have been mentioned by Wolf in Solid State Physics, Vol. 9, but these data have not been taken notice of in the volumes under review.

Nevertheless, the publication of the volumes will enable a large number of research workers all over the world to save their valuable time in procuring the

data and will thus hasten the progress of research in chemistry and some branches of physics. It is stated in the Introduction of Vol. II that the next three volumes are in preparation. It is fervently hoped that the above remarks regarding omission of certain data will be taken notice of by the Board of Editors before the next three volumes are published.

The get-up of the volumes is excellent and in view of the fact that the co-operation of a large number of specialists has been required to publish the volumes the prices are considered to be quite moderate.

S. C. S.

IMPORTANT PUBLICATIONS

The following special publications of the Indian Association for the Cultivation of Science, Jadavpur, Calcutta, are available at the prices shown against each of them:—

TITLE	AUTHOR	PRICE
Magnetism ... Report of the Symposium on Magnetism		Rs. 7 0 0
Iron Ores of India	... Dr. M. S. Krishnan	5 0 0
Earthquakes in the Himalayan Region	... Dr. S. K. Banerji	3 0 0
Methods in Scientific Research	.. Sir E. J. Russell	0 6 0
The Origin of the Planets	.. Sir James H. Jeans	0 6 0
Active Nitrogen— A New Theory.	.. Prof. S. K. Mitra	2 8 0
Theory of Valency and the Structure of Chemical Compounds.	.. Prof. P. Ray	3 0 0
Petroleum Resources of India	.. D. N. Wadia	2 8 0
The Role of the Electrical Double-layer in the Electro-Chemistry of Colloids.	.. J. N. Mukherjee	1 12 0
The Earth's Magnetism and its Changes	.. Prof. S. Chapman	1 0 0
Distribution of Anthocyanins	.. Robert Robinson	1 4 0
Lapinone, A New Antimalarial	.. Louis F. Fieser	1 0 0
Catalysts in Polymerization Reactions	.. H. Mark	1 8 0
Constitutional Problems Concerning Vat Dyes.	.. Dr. K. Venkataraman	1 0 0
Non-Aqueous Titration	.. Santi R. Palit, Mihir Nath Das and G. R. Somayajulu	3 0 0
Garnets and their Role in Nature	.. Sir Lewis L. Fermor	2 8 0

A discount of 25% is allowed to Booksellers and Agents.

NOTICE

No claims will be allowed for copies of journal lost in the mail or otherwise unless such claims are received within 4 months of the date of issue.

RATES OF ADVERTISEMENTS

1. Ordinary pages:
   - Full page .. .. Rs. 50/- per insertion
   - Half page .. .. Rs. 28/- per insertion
2. Pages facing 1st inside cover, 2nd inside cover and first and last page of book matter:
   - Full page .. .. Rs. 55/- per insertion
   - Half page .. .. Rs. 30/- per insertion
3. Cover pages .. .. by negotiation

25% commissions are allowed to *bona fide* publicity agents securing orders for advertisements.

CONTENTS

Indian Journal of Physics Vol. 35, No. 5 May, 1961

PRINTED BY KALIPADA MUKHERJEE, EKA PRESS, 204/1, B. T. ROAD, CALCUTTA-35
PUBLISHED BY THE REGISTRAR, INDIAN ASSOCIATION FOR THE CULTIVATION OF SCIENCE
2 & 3, LADY WILLINGDON ROAD, CALCUTTA-32